HADRONIC PRODUCTION OF MASSIVE DIMUON AT CERN-SPS

reported by P. LE DÛ

CEN-Saclay, DPhPE, France

SLAC Summer institute on particle physics.
Stanford, USA, July 9 - 20, 1979.
CEA - CONF 5000

This talk presents the first results of the NA3-LEZARD experiment which is a collaboration between :

CERN : D. Décamp, R. Hagelberg, M. Hansroul, W. Kienzle, G. Matthiae, A. Michelini, O. Runolfsson, J. Timmermans, S. Weisz.

COLLEGE de FRANCE : M. Crozon, P. Delpierre, A. Diop, J. Valentin, T. Leray.

ORSAY : J. Boucrot, O. Callot, R. Dubé, J. Lefrançois, H. Nguyen Ngoc.

ECOLE POLYTECHNIQUE : J. Badier, P. Minè, R. Vanderhagen.

SACLAY : G. Burgun, P. Charpentier, B. Gandois, A. La Fontaine, P. Le DÛ, P. Siegrist.

ABSTRACT :

The aim of this experiment is to study massive muon pairs produced by π^- at 280 GeV/c and $\pi^\pm$, $K^\pm$, p and $\bar{p}$ at 200 GeV/c on platinum and hydrogen targets. Results are presented on :

A/ Vector mesons production through their μ pair decay mode like :

- low mass resonances (ρ, ω, φ) at high transverse momentum.
- φ/J production and its X, p_t, $\cos\theta^*$ distributions.
- First evidence for Υ production by 200 and 280 GeV/c pions.

B/ High mass continuum. A total of more than 10 000 dimuon events of Drell-Yan type ($M_{\mu\mu} > 4$ GeV/c^2) are analyzed giving results on nuclear target and p_t dependence, decay angular distribution, absolute comparison of $\pi^\pm$, $K^\pm$, p, $\bar{p}$ induced mass spectra, scaling.

I EXPERIMENTAL FEATURES :

I.1 Beam parameters

The incident beam is the CERN SPS-H8 unseparated secondary hadron particle beam produced by protons of 400 GeV/c on a 50 cm Be target. We ran at two momenta : 200 and 280 GeV/c. The particle identification (only for 200 GeV/c) is done by two differential Cerenkov counters (CEDAR's) [1] for $K^\pm$, $\bar{p}$ and two threshold Cerenkov counters for $\pi^\pm$. The particle fluxes were in the range (1 - 3).10^7 part./pulse. Contents of

the 200 GeV/c tagged beam are given in the following table :

P inc [%]	π	K	P
- 200 GeV/c	96.3	3.1	0.62
+ 200 GeV/c	36.	4.6	59.4

A 2m long CH_2 absorber was used to enhance the π^+ percentage of the positive beam from 20 % to about 36 %.

I.2 Detector layout

The experiment was performed in the LEZARD-NA3 large acceptance spectrometer in a beam dump configuration [2]. The general layout of the apparatus is shown in fig. 1a.

Platinum targets, 6cm long for 200 GeV run and 11.1cm for the 280 GeV run, were used. At 200 GeV we have also used simultaneously a 30 cm long liquid hydrogen target.

After passing through the targets, the beam is absorbed in a dump which starts 40 cm downstream of the Pt target. It consists of a 1.5 long block of stainless steel with a heavy (tungsten and uranium) conical plug of $\pm$ 30 mrad aperture inserted in the center, in order to minimize the total beam dump lengh.

The large acceptance magnetic spectrometer LEZARD consists of :

(i) a large superconducting dipole magnet with a vertical field ($\int Bdl = 4.0$ Tm) in an airgap of cylindrical useful aperture of 1.6m diameter. [3]

(ii) a set of six multiwire proportional chambers (31 planes

ing table :

he π^+ per-
6 %.

NA3 large
tion [2].
ig. 1a.
and 11.1cm
ve also used
et.
is absorbed
t target. It
with a heavy
aperture
total beam

LEZARD consists

a vertical
indrical

rs (31 planes

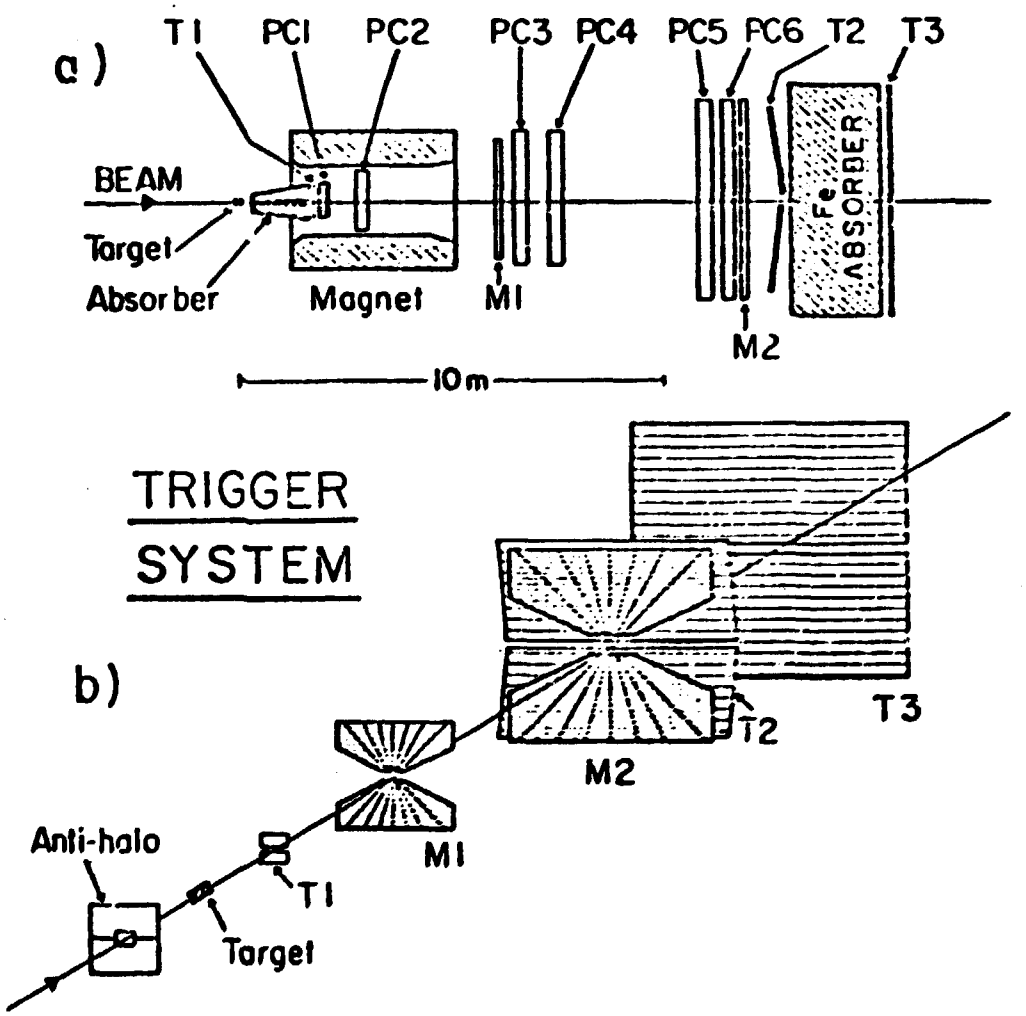

FIG. 1

(a) General layout of the NA3 spectrometer for the study of dimuon production in hadronic collisions. T1, T2, T3 : counter hodoscopes ; M1, M2 : trigger chambers ; PC1-6 : proportional chambers.

(b) Sketch of the trigger system. The azimuthal subdivision of M1 and M2 (64 cells) is much finer than indicated.

with a total of about 26 000 wires) ranging in size from $0.6 \times 0.6 m^2$ (PC1) up to $4.2 \times 4.0 m^2$ (PC6) ;

(iii) muon filtering, behind the beam dump, is provided by 12 cm of lead, and 1.8 m of iron, placed in front of the last triggering hodoscope T3 ;

(iv) the trigger system consists of two symmetric telescopes of counters and chambers placed above and below the horizontal plane.

I.3 Trigger system

The study of very low cross section process ($\leq 10^{-33} cm^2$) like massive muon pairs production requires a high rejection rate (10^{-6}). A very selective trigger is made in two steps.

a) The PRETRIGGER

This first level requires geometrical conditions involving three planes of counter hodoscopes :

- presence of at least two muons in the final state. For that, we use a correlation in the vertical plane, between horizontal slabs of the back hodoscopes T2 and T3 in order to constraint each muon to point approximatively towards the targets region inside a lot of 22 roads ;
- muon halo cut off by veto counters before the spectrometer ;
- hit in the T1 counters, placed at the end face of the beam dump, for timing reference.

The two hodoscopes T2 and T3 cover vertical angles from $\pm$ 6 mrad up to $\pm$ 165 mrad. The PRETRIGGER provides a fast

strobe for the proportional chambers PC1, PC2, M1 and M2 in order to minimize electronics dead-time due to the high particle flux.

b) The trigger

The final trigger acts on the vertical component p_t^v of the transverse momentum of the muons. The p_t^v selection is achieved by two homothetical planes of cathode-readout chambers M1 and M2 covering vertical angles from $\pm$ 30 mrad up to $\pm$ 165 mrad. The mylar cathode planes are graphite coated in 18 separated horizontal strips, each subdivised into 64 cells corresponding to equal intervals of the tangent of the azimuthal angle. The correlation between cells of a given strip provides a cut-off in the magnetic deflection angle and thus p_t^v, with in turn, defines a rough lower cut in the muon pair effective mass. The trigger conditions in the course of the experiment were :

- either $p_t^v > 1$ GeV/c for one muon, without cut on the other muon (trigger I) ;
- or $p_t^v > 0.7$ GeV/c for both muons (trigger II).

Events with both muons in the 30 mrad cone of the W/U core of the beam dump were not accepted. Typical trigger rate was 30 events/pulse corresponding to 1 ψ recorded per pulse of 1 second. The trigger system is illustrated in fig. 1b.

I.4 Acceptance

The overall acceptance of the apparatus, as determined by the geometry of the detectors and by the p_t^v cut is shown in fig. 2 as a function of the dimuon mass, the transverse

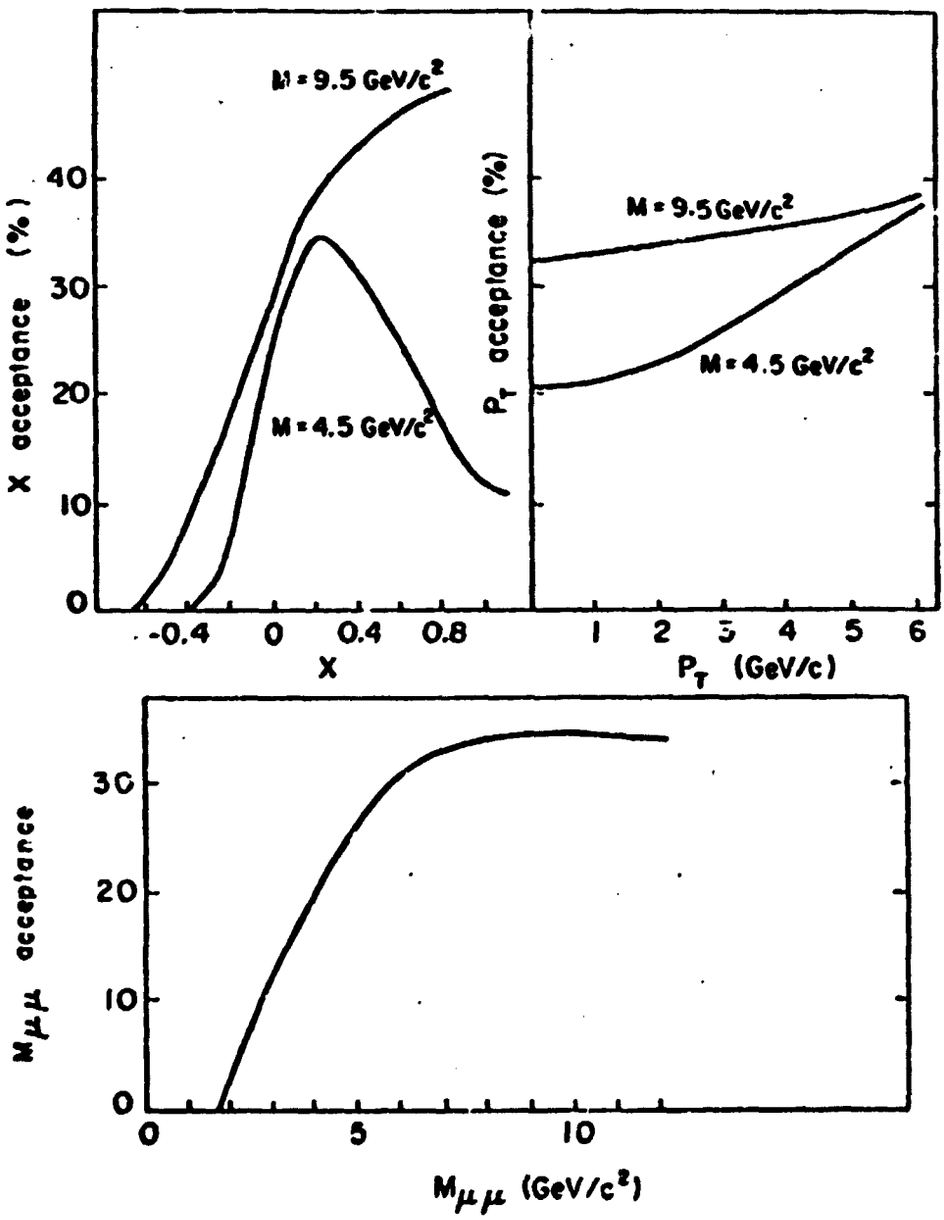

Acceptance 200 GeV/c

FIG. 2

Acceptance of the apparatus, as a function of $x = 2 P_L^*/\sqrt{s}$, of the transverse momentum p_t and of the dimuon mass M.

momentum of the pair and the variable $x = 2\,p_L^*/s$, (where p_L^* is the longitudinal momentum of the dimuon in the c.m. system, $\sqrt{s}$ the total energy). The resolution at the ψ mass is $\pm$ 5 % decreases, slightly towards $\pm$ 3 % at the T mass (dominated by momentum resolution).

I.5 Data taking and analysis

Between September 1978 and April 1979 were recorded and analyzed a total of 10^7 triggers. Pattern recognition of both muons is performed in the spectrometer chambers with an overall efficiency of 94 % $\pm$ 2 %, measured from visual scanning of a sample of reconstructed events. Vertex reconstruction is done taking into account multiple scattering in the hadron absorber and beam constraint at the target. For dimuon events with a mass above 4 GeV/c^2, the distribution of reconstructed vertex position (fig. 3) shows a clean separation between interactions in the hydrogen target, the platinum target and the beam dump.

II RESONANCES PRODUCTION :

II.1 Low mass vector mesons : [4]

Due to the fact that our trigger conditions are quite inefficient (< 5 %) for such low masses with p_t < 1.5 GeV/c we concentrated our study on muon pairs of p_t greater than 2.0 GeV/c for masses between 0.4 and 2.0 GeV/c^2. The fig. 4 shows the mass spectra for incident π^+'s and K^+'s. Background from π decays are estimated from like sign pairs to be less than 1 % in this range.

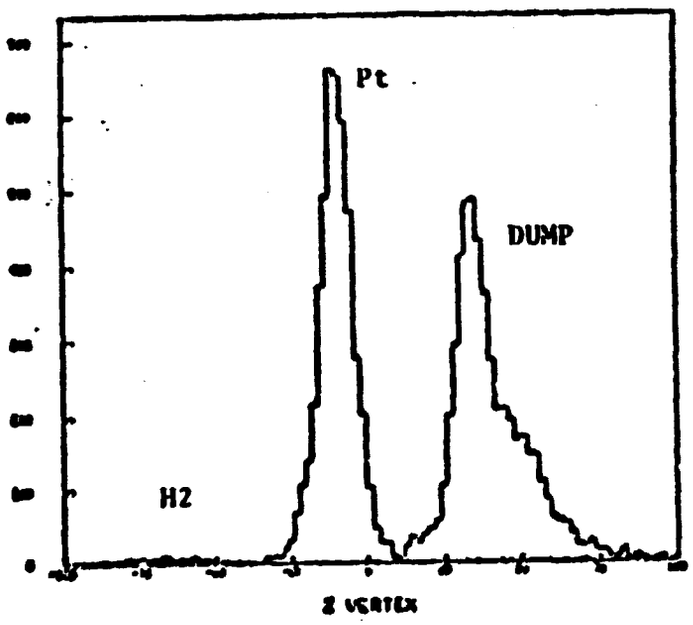

a) Linear scale

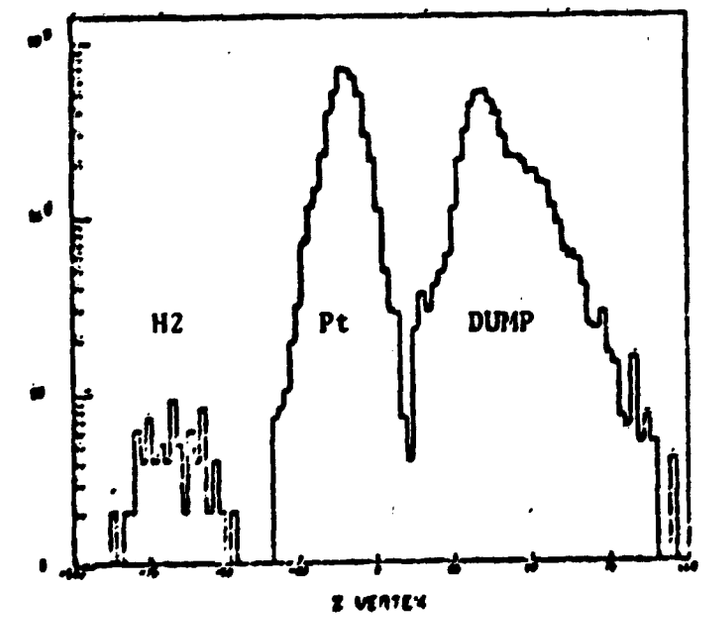

b) Log. scale

Fig. 3

Reconstructed dimuon vertex

II.1.1

The

assumpti

(i) a μ

(ii) thr

width of

the same

section

As

and the

of this

λ (G
0.661

In

their c

spectra

spectra

200 Ge

The cr

$\mu^+\mu^-$ b

II.1.1 Comparison between ρ, ω and ϕ production :

The mass spectra are fitted using the following assumptions :

(i) a $\mu^+\mu^-$ continuum parametrized as $e^{-M/\lambda}$;

(ii) three resonances : ρ°, ω, ϕ assuming $m_\rho = m_\omega$, a natural width of 155 MeV for ρ°, no interference between ρ° and ω, the same resolution δ for each resonance, and equal cross section for ρ° and ω production.

As a first step, we use m_ρ, m_ϕ, δ, λ, $R_{\phi\rho} = B\sigma(\phi)/B\sigma(\rho^\circ)$ and the fraction of continuum as free parameters. The result of this fit for incident π^+'s gives :

λ (GeV/c^2)	M_ρ (MeV/c^2)	M_ϕ (MeV/c^2)	δ (MeV/c^2)	$R_{\phi\rho}$	χ^2/D.F.
0.661 ± 0.016	791.8 ± 3.5	1037 ± 6.	109.5 ± 3.0	0.86 ± 0.04	37.5/33

In a second step we have fixed the resonance masses to their canonical value, and the resolution (δ) for kaon induced spectra is taken to be the mean value of π^+ and π^- induced spectra i.e. 108 MeV/c^2. The fitted parameters for incident 200 GeV/c $\pi^\pm$, $K^\pm$ and protons are given in the following table. The cross section ratio of ϕ relative to ρ°, takes into account $\mu^+\mu^-$ branching ratios i.e.

$$\frac{B(\phi \to \mu^+\mu^-)}{B(\rho^\circ \to \mu^+\mu^-)} = 7.21 \pm 0.87$$

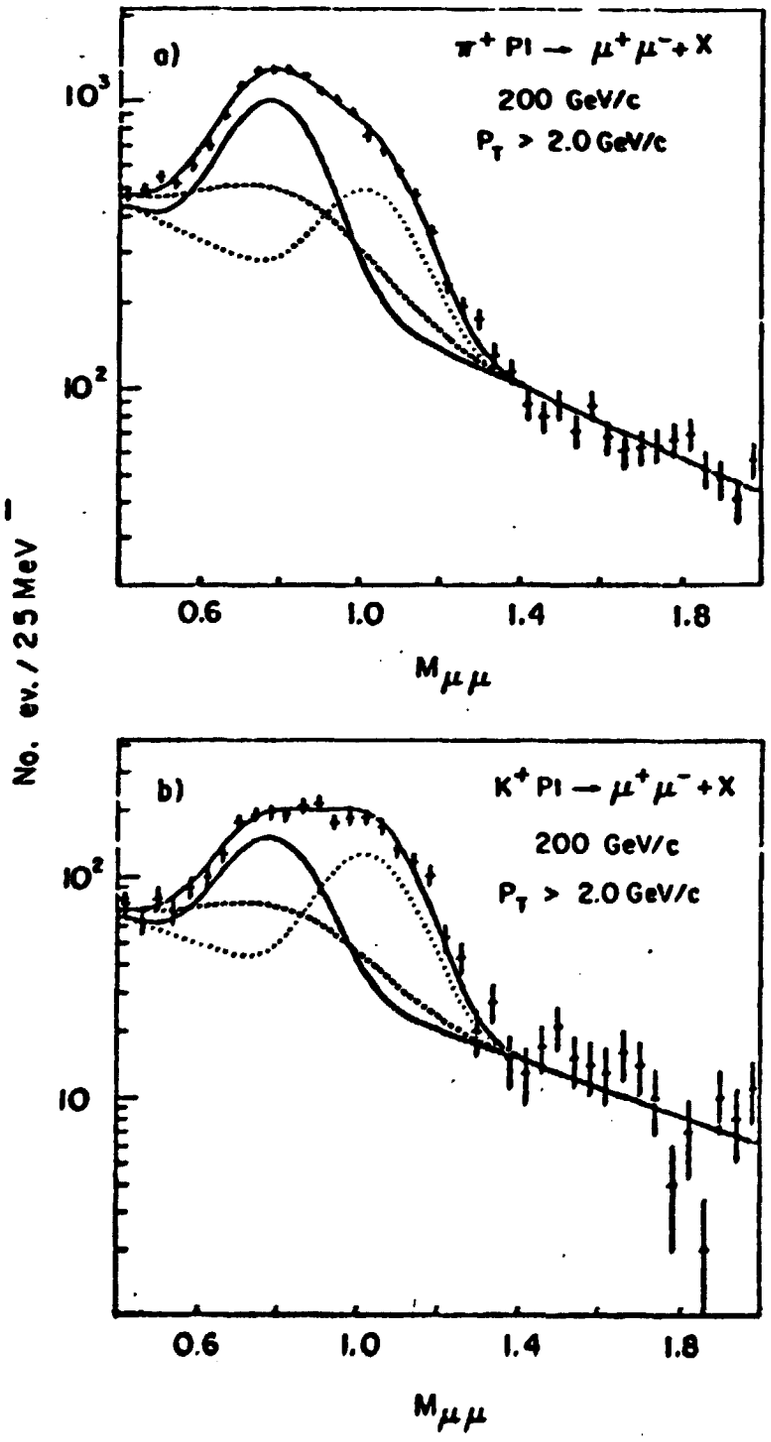

FIG. 4

Mass spectrum in the ρ^o, ω, ϕ region with p_t > 2 GeV/c for a) Incident π^+, b) Incident K^+.

P_{inc}	p_t	λ (GeV/c^2)	δ (MeV/c^2)	$R_{\phi\rho}$	χ^2/D.F.	$\frac{\sigma(\phi)}{\sigma(\rho)}$ [%]
p	> 2.	0.607 ±0.012	102.4 ± 2.6	0.86 ± 0.03	47.3/35	11.9 ± 1.5
	> 3.	0.66 ±0.05	108*	1.04 ± 0.13	25.2/36	14.4 ± 2.5
π^+	> 2.	0.687 ±0.018	110.5 ± 3.4	1.05 ± 0.05	49.8/35	14.6 ± 1.9
	> 3.	0.83 ± 0.08	108*	1.33 ± 0.16	56/36	18.5 ± 3.2
K^+	> 2.	0.67 ± 0.04	108*	2.25 ± 0.16	64/36	31.2 ± 4.4
π^-	> 2.	0.84 ± 0.02	106.0 ± 3.0	1.11 ± 0.04	53/35	15.4 ± 2.0
	> 3.	0.74 ± 0.04	108*	1.54 ± 0.17	65.7/36	21.4 ± 3.5
K^-	> 2.	0.70 ± 0.09	108*	2.46 ± 0.50	33.2/36	34.1 ± 8.1

* Fixed parameter

One can see that the relative production $R_{\phi\rho}$ is about two times larger for kaonsthan for pions or protons. This is qualitatively expected from quark contents, since kaons have strange valence quarks. But this ratio does not seem to decrease as p_t increases, like would be expected from a quark scattering model.

II.1.2 Cross section and p_t dependence :

From the relative particle content of our beam (known from Cerenkov's within 10 %) we can compute the cross section ratios for different incident hadrons independently of acceptance corrections (if p_t distributions are not too different).

	π^+	K^+	K^-	p
$\frac{\sigma(X\,Pt \to \rho^0)}{\sigma(\pi^- Pt \to \rho^0)}$	1.12 ± 0.07	0.85 ± 0.10	0.94 ± 0.11	0.11 ± 0.13
$\frac{\sigma(X\,Pt \to \phi)}{\sigma(\pi^- Pt \to \phi)}$	1.06 ± 0.07	1.75 ± 0.10	2.11 ± 0.24	0.86 ± 0.10

> 2 GeV/c

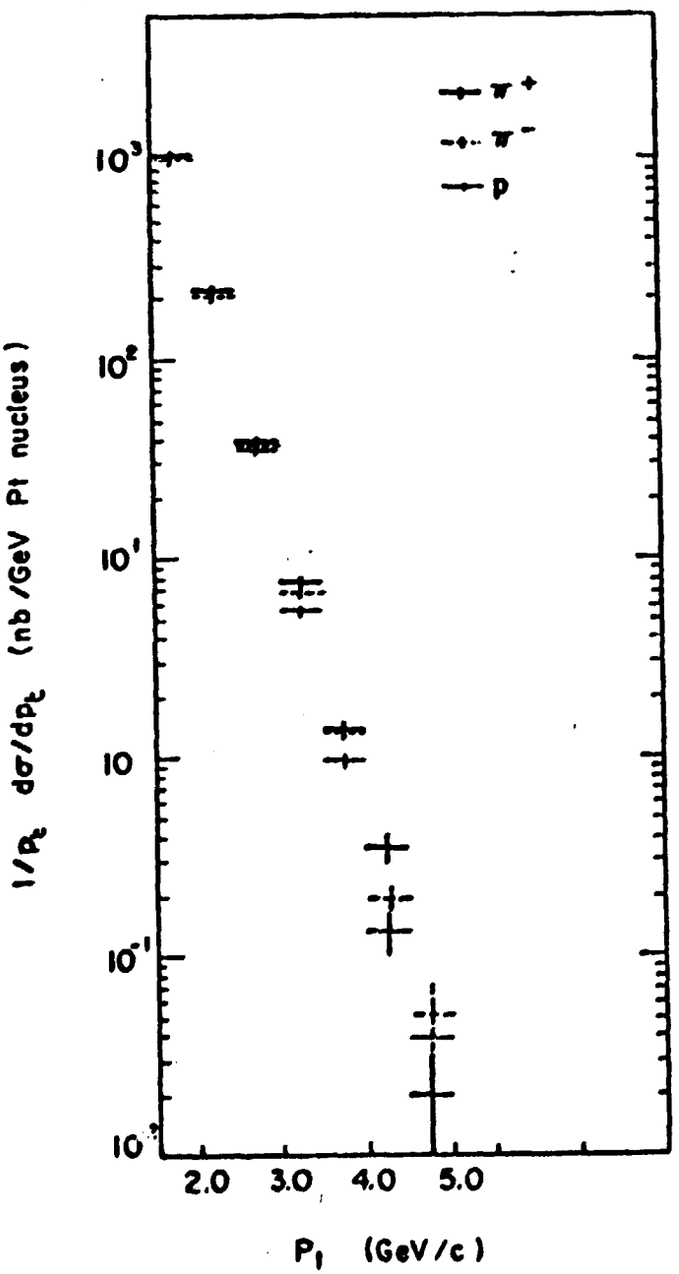

FIG. 5

$1/p_t\ d\sigma/dp_t$ for masses between 0.6 GeV/c^2 and 1.0 GeV/c^2

For p
increases
incident
interval
shown. Sy
are estim

The
form :

Thi
are in g
ρ^0 and ω
smaller

II.2 J/

We
dimuon d
and two
cative s
K^+ and
followi

For p_t > 2 GeV/c, our acceptance is around 10 %, and increases with p_t. The p_t differential cross sections for incident π^+, π^- and protons are shown in fig. 5 for a mass interval from 0.6 to 1.0 GeV/c^2. Only statistical errors are shown. Systematic errors on normalization, acceptance etc... are estimated to about 20 %.

The p_t distribution is well fitted by the parametrized form :

$$\frac{1}{p_t}\frac{d\sigma}{dp_t} \propto e^{-(3.2 \pm 0.2)p_t}$$

This slope value, as well as the absolute cross section are in good agreement with Anderson et al. [5] who measured ρ° and ω production by 150 GeV/c pions and protons for p_t smaller than 2 GeV/c.

II.2 J/ψ Production

We have recorded a large sample of J/ψ events in their dimuon decay mode (fig. 6) with different incident particles and two targets simultaneously. For the first time significative statistics were observed on hydrogen with p, π^+, π^-, K^+ and on platinum with π^+, K^+, K^- and $\bar{p}$ as reported in the following table :

P_{inc}		Platinum	Hydrogen
280 GeV/c	π^-	130 000	-
200 GeV/c	π^-	145 000	3 000
	K^-	2 800	56
	$\bar{p}$	1 000	17
200 GeV/c	π^+	108 000	2 200
	K^+	16 000	340
	p	101 000	2 300

0 GeV/c^2

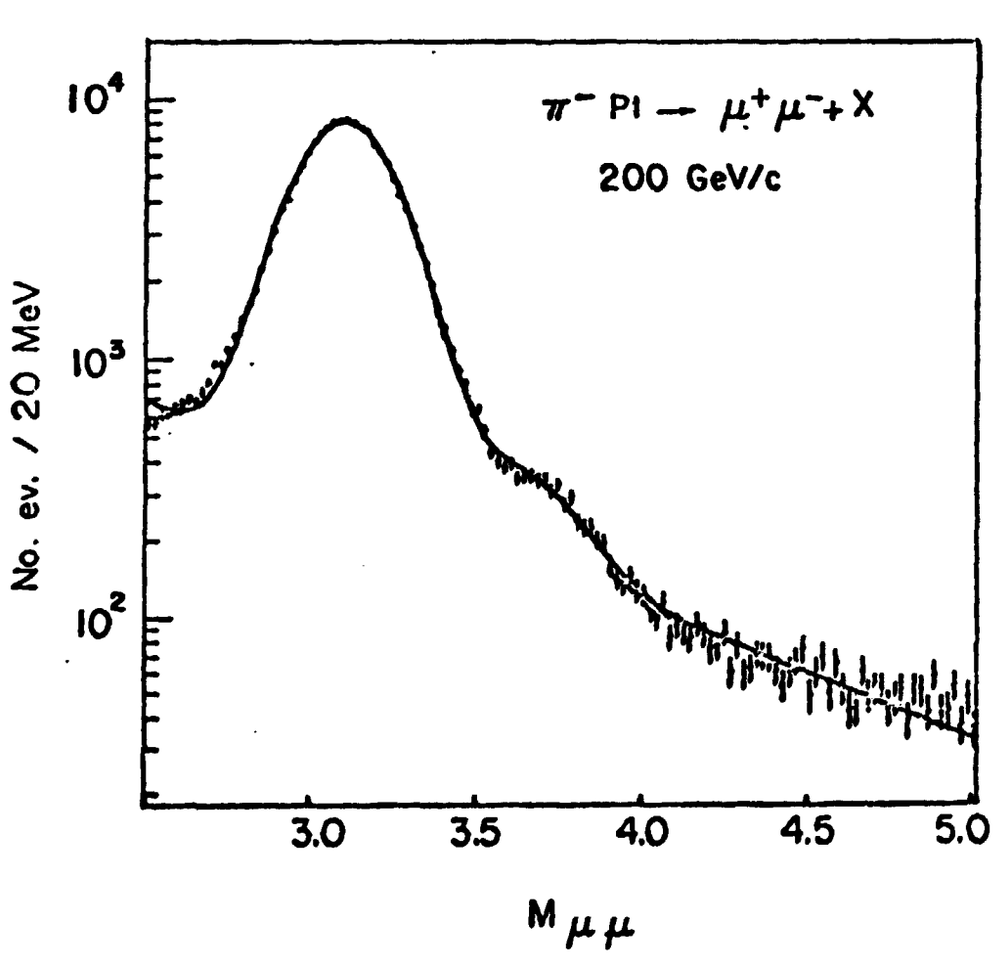

FIG. 6

Mass spectrum for J/ψ events from incident 200 GeV/c π^-'s

II.2.1

We

platinum

we can d

of absol

taneousl

R_π

Tho

correcti

Ass

Tal

tinum t

R

Th

which i

Th

the sys

r_{pt}.

II.2.2

Th

have b

II.2.1 Comparison of J/ψ production by π^+ and π^- on protons :

We have used our 200 GeV/c data on both hydrogen and platinum targets. From the number of events on each target, we can deduce two ratios R_{π^+} and R_{π^-} which are independent of absolute normalization, as both targets are used simultaneously

$$R_{\pi^-} = \left(\frac{\psi_{H_2}}{\psi_{Pt}}\right)_{\pi^-} = 0.0209 \qquad R_{\pi^+} = \left(\frac{\psi_{H_2}}{\psi_{Pt}}\right)_{\pi^+} = 0.0205$$

The ratio $R = R_{\pi^+}/R_{\pi^-}$ is then independent of acceptance corrections. One gets $R = 0.98 \pm 0.03$.

Assuming isospin invariance let us call :

$$\sigma^+ = \sigma(\pi^+ p \to \psi \ldots) = \sigma(\pi^- n \to \psi \ldots)$$
$$\sigma^- = \sigma(\pi^- p \to \psi \ldots) = \sigma(\pi^+ n \to \psi \ldots)$$

Taking into account the fraction of neutron in the platinum target ($Z/A = 0.40$), the ratio R can be written as :

$$R = \frac{\sigma^+}{0.4\,\sigma^+ + 0.6\,\sigma^-} \Big/ \frac{\sigma^-}{0.4\,\sigma^- + 0.6\,\sigma^+}$$

This equation allows to determine the ratio

$$r_{H_2} = \sigma^+/\sigma^- = 0.987 \pm 0.02$$

which implies $r_{Pt} = \dfrac{\sigma(\pi^+ Pt \to \psi \ldots)}{\sigma(\pi^- Pt \to \psi \ldots)} = 1.003 \pm 0.004$.

The errors given here are statistical only, we estimate the systematic error to be less than 5 % on r_{H_2} and 1 % on r_{Pt}.

II.2.2 Total cross section and A dependence

The total cross section and the cross section for $x > 0$ have been evaluated from a clean sample of our J/ψ events

for 200 GeV/c and 280 GeV/c incident π's. They have been corrected for reinteraction in the platinum target, measured to be 10 % at 200 GeV/c in a 6cm target, and 19 % at 280 GeV/c in a 11cm target. The results are given in μb/Pt nucleus (A = 195).

P_{beam}	200 GeV/c	280 GeV/c
Part.	π^-	π^-
σ_{tot}	1.56 ± 0.27	2.12 ± 0.47
$\sigma(x > 0)$	0.76 ± 0.14	1.05 ± 0.24

Relative cross sections for other particles have been determined from Cerenkov's informations (known to about 10 %). Calibration between positive and negative beams in made using our r_{p_t} ratio

P_{beam}	200 GeV/c				
Part	K^-	$\bar{p}$	π^+	K^+	p
$\frac{\sigma_{tot}(x)}{\sigma_{tot}(\pi^-)}$	1.1 ± 0.1	0.83 ± 0.12	1.01 ± 0.02	0.78 ± 0.08	0.59 ± 0.10

From these values we can deduce the ratios :

$$\frac{\sigma(\bar{p}\,Pt \to \psi \ldots)}{\sigma(p\,Pt \to \psi \ldots)} = 1.4 \pm 0.2 \qquad \text{and} \qquad \frac{\sigma(K^-\,Pt \to \psi \ldots)}{\sigma(K^+\,Pt \to \psi \ldots)} = 1.4 \pm 0.2$$

showing that qualitatively, part of the ψ are produced by valence quark interactions.

Combining the data obtained on hydrogen and platinum targets, we may estimate the mass dependence of ψ production. Experimentally, the ratio $\frac{A\sigma(\pi^- H_2 \to \psi)}{\sigma(\pi^- Pt \to \psi)} = 1.31 \pm 0.18$. Assuming for the A dependence the power law A^α we get

$M^2 \sigma_{tot}$ (nb / nucleon) x GeV^2

100

10

ave been
et, measured
% at 280
μb/Pt nu-

have been
o about 10 %).
in made using

	p
8	0.59 ± 0.10

= 1.4 ± 0.2

duced by

d platinum
ψ produc-
1.31 ± 0.18.
ve get

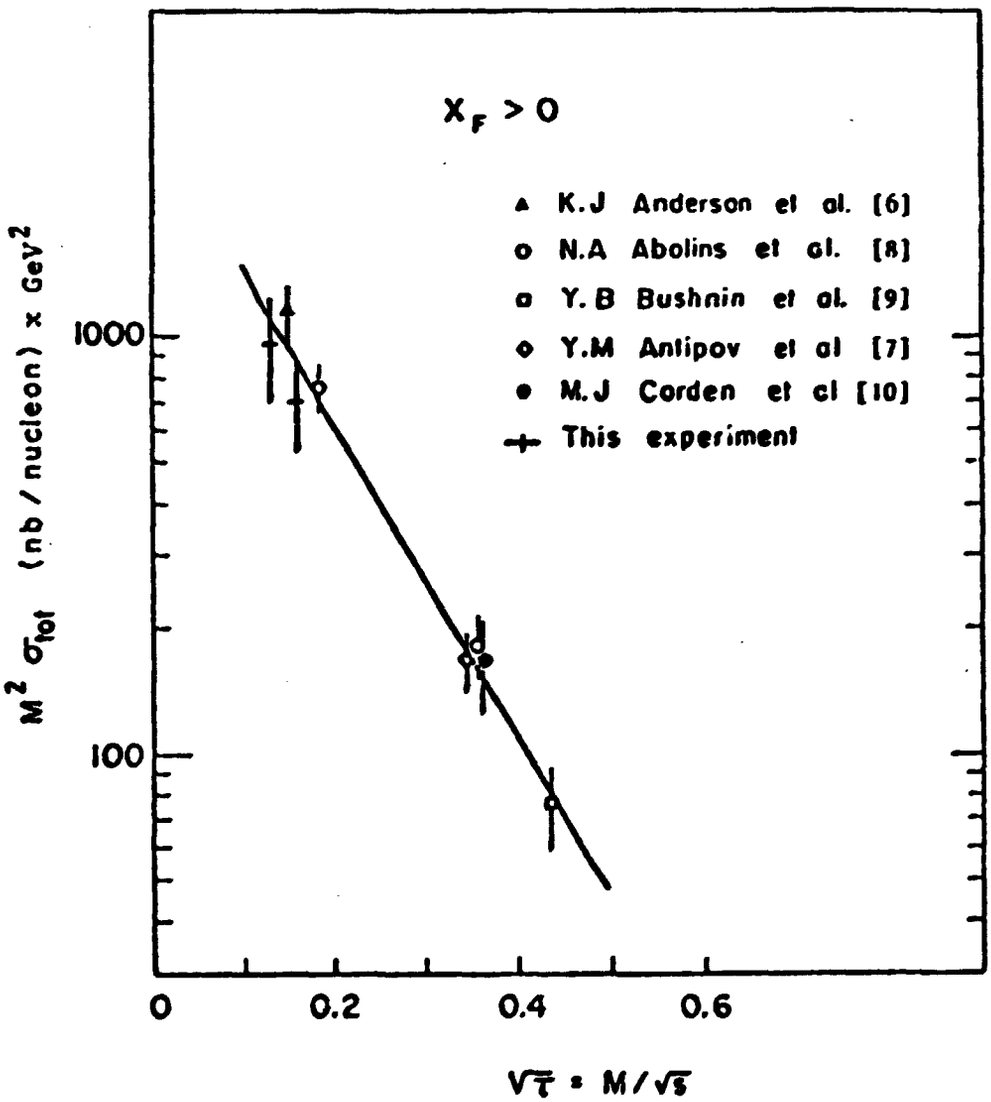

FIG. 7

J/ψ excitation curve for incident pions

$\alpha = 0.95 \pm 0.03$ which is in good agreement with previous measurements.

References	P_{inc}	α	α average
Anderson et al. [6]	225 GeV/c	0.87 ± 0.05	
Antipov et al. [7]	43 GeV/c	0.92 ± 0.06	0.927 ± 0.030
This experiment	200 GeV/c	0.95 ± 0.03	

Using our measured value of α, we have plotted in fig. 7 $M^2\sigma_{tot}(\pi^- N \to \psi \ldots)$ as a function of $M/\sqrt{s}$ for different experiments.

II.2.3 x distribution of J/ψ

Fig. 8 shows the acceptance of our apparatus as a function of x and the differential cross section $d\sigma/dx$ for π^- induced J/ψ events. The acceptance is computed by Monte Carlo method assuming an isotropic decay distribution of the muons in the J/ψ rest frame (see sect. II.2.5). For $x \geq 0.2$ the experimental distribution has been fitted to a form $(1-x)^n$ with $n = 2.98 \pm 0.03$.

The ratio $\dfrac{d\sigma/dx\ (X\,Pt \to \psi \ldots)}{d\sigma/dx\ (\pi^{\pm} Pt \to \psi \ldots)}$ is presented in Fig. 9 for different incident particle X. Relative normalization between positive and negative beams is made using our result $\sigma(\pi^+ Pt \to \psi \ldots) = \sigma(\pi^- Pt \to \psi \ldots)$ (within 1 %). The normalization of $K^{\pm}$, $\bar{p}$ and protons are known within 10 %. Error bars do not include this systematic error.

The x distributions of all meson induced reactions are similar and somewhat flat. That can be interpreted as the constituent distribution in the kaons and in the pions have

previous

erage
± 0.030

d in fig. 7
different

atus as a func-
dσ/dx for π⁻
ed by Monte Carlo
ion of the muons
x ≥ 0.2 the
a form $(1-x)^n$

ted in Fig. 9
normalization
using our result
%). The normali-
10 %. Error bars

reactions are
preted as the
n the pions have

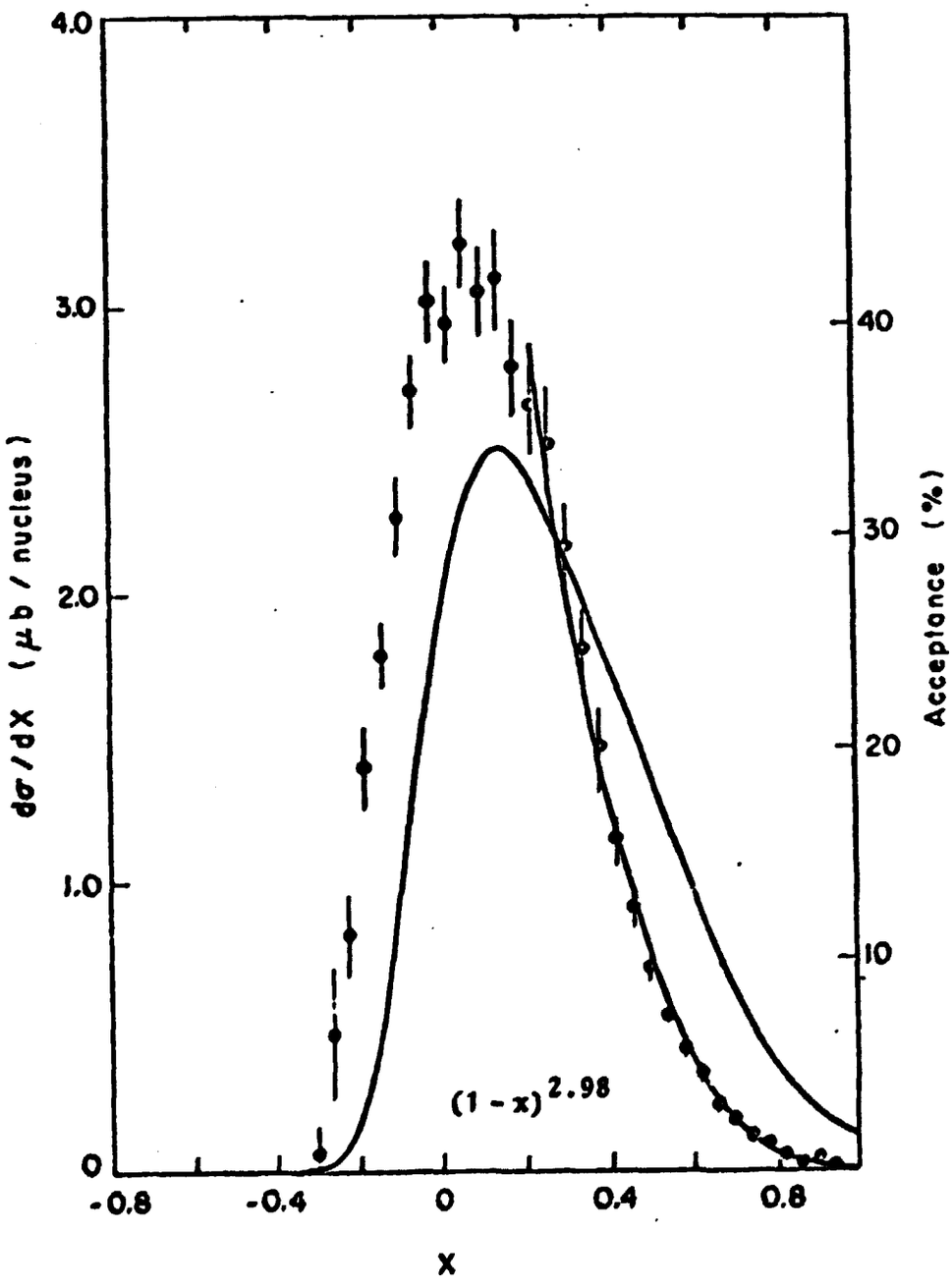

FIG. 8

x acceptance for J/ψ and differential cross section dσ/dx for incident π⁻'s at J/ψ

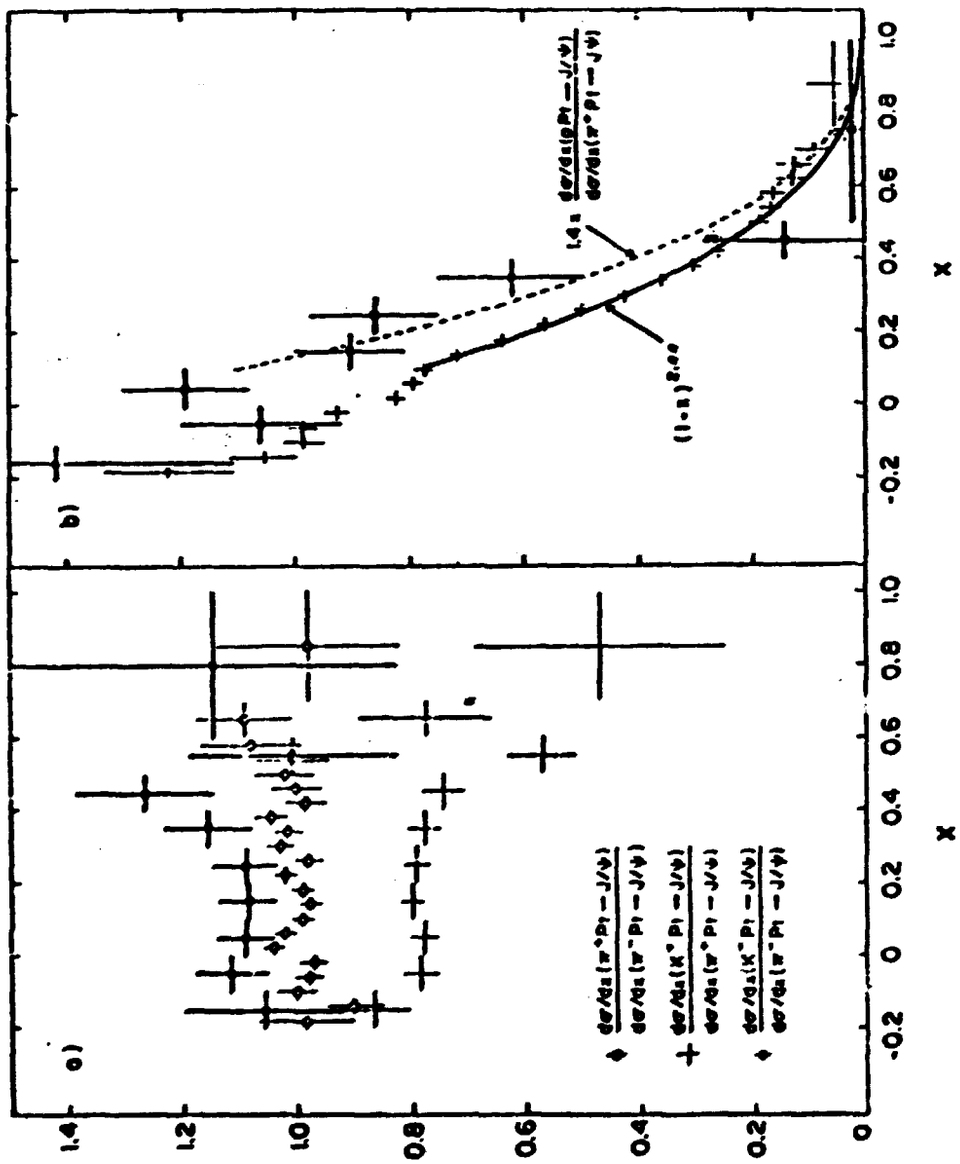

FIG. 9

Ratio of dσ/dx for different particles over dσ/dx for incident pions. a) Incident mesons, b) Incident baryons

the same b
function).

Objec
fall off w
$R_p(x)$ has
easily be
butions in
structure

II.2.4 Th

Diffe
are shown
momentum.

These
by a funct
reported
Our distr

$$\frac{1}{p_t}\frac{d}{d}$$

γ has fir
ratio of
Fixing m
neous fit
a χ^2 of 1
are shown
leads to
and the χ

the same behaviour in x (i.e. the same shape of the structure function).

Objet to, the baryons induced reactions show a steep fall off with x, similar for p and $\bar{p}$. At large x (> 0.1), $R_p(x)$ has been fitted by $(1-x)^{2.45 \pm 0.07}$. This ratio can easily be interpreted as the ratio of constituents distributions in protons and in pions, falling as $(1-x)^m$ (from structure functions), with m between 2 and 3.

II.2.4 Transverse momentum p_t distribution of J/ψ

Differential cross sections $1/p_t \, d\sigma/dp_t$ ($\pi^- Pt \to \psi \ldots$) are shown in fig. 10 at 200 GeV/c and 280 GeV/c incident momentum.

These cross section are not well fitted above 4 GeV/c by a function of the form $(1 - p_t^2/m^2)^{-6}$ as was previously reported [8, 11] neither with a simple gaussian $\exp(-p_t^2/a^2)$. Our distributions are fitted with a form :

$$\frac{1}{P_t}\frac{d\sigma}{dp_t} \propto (1-x_t)^{\gamma} \left(1+\frac{p_t^2}{m^2}\right)^{\beta} \quad \text{where} \quad x_t = \frac{2P_t}{\sqrt{s}}$$

γ has first been determined by a least square fit to the ratio of the two p_t distributions. We find γ to be 5.56 ± 0.50. Fixing m at the ψ mass, one get a value of β from a simultaneous fit of 200 and 280 GeV/c data : $\beta = -4.86 \pm 0.02$ with a χ^2 of 153 for 123 degrees of freedom. The resulting curves are shown in fig. 10. Now, leaving m as a free parameter leads to the result $\beta = -6.01 \pm 0.13$, $m = 3.66 \pm 0.10$ GeV/c^2 and the χ^2 becomes 106 for 122 degrees of freedom.

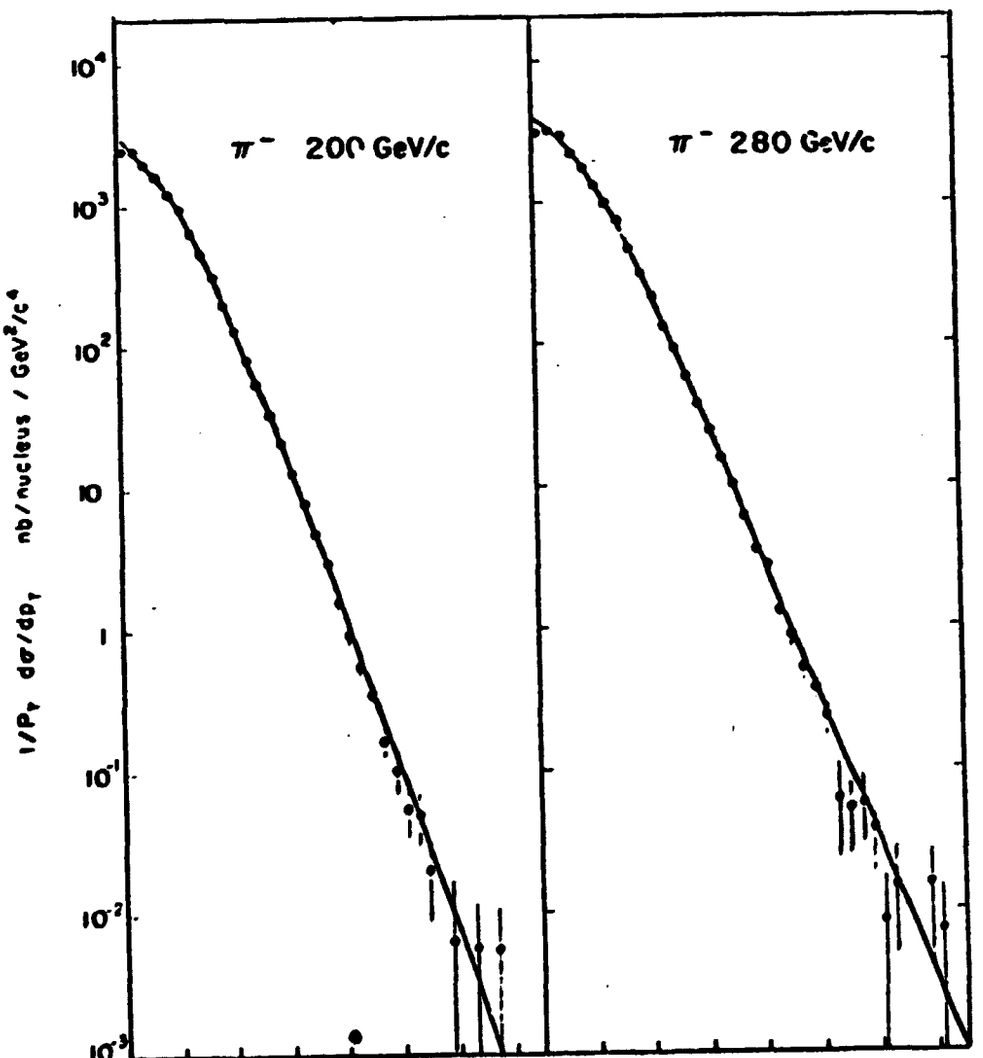

FIG. 10

$1/p_t\ d\sigma/dp_t$ ($\pi^- p_t \to J/\psi$) for 200 GeV/c and 280 GeV/c pions

The following table summarises the results for the average $< p_t >$ and $< p_t >^2$. One can observe that the $< p_t >$ increases with energy and it is greater for the mesons than for the baryons.

P_{inc}		$< p_t >$	$< p_t >^2$
280 GeV/c	π^-	1.18 ±0.01	1.86 ±0.02
200 GeV/c	π^-	1.12 ±0.01	1.70 ±0.03
	K^-	1.13 ±0.04	1.69 ±0.10
	$\bar{p}$	1.05 ±0.06	1.50 ±0.20
	π^+	1.12 ±0.01	1.66 ±0.03
	K^+	1.14 ±0.03	1.75 ±0.10
	p	1.07 ±0.01	1.52 ±0.02

II.2.5 Angular distribution of muons :

The study of angular distribution of muons in the ψ frame gives information about its production mechanism. The choice of the axis depends on the production model. In the Gottfried-Jackson frame, for example, the angular distribution has the form :

$$\frac{d\sigma}{d\cos\theta_{GJ}} = A\,(1 + \lambda\cos^2\theta_{GJ})$$

In a quark fusion model producing directly the J/ψ, λ is given by

$$\lambda = \frac{1 - 4m^2/Q^2}{1 + 4m^2/Q^2} \qquad \text{ref. [8]}$$

The cross section as a function of the Gottfried-Jackson angle is given in fig. 11 for incident 200 GeV/c π^-'s, in the mass range 2.7 to 3.5 GeV/c^2.

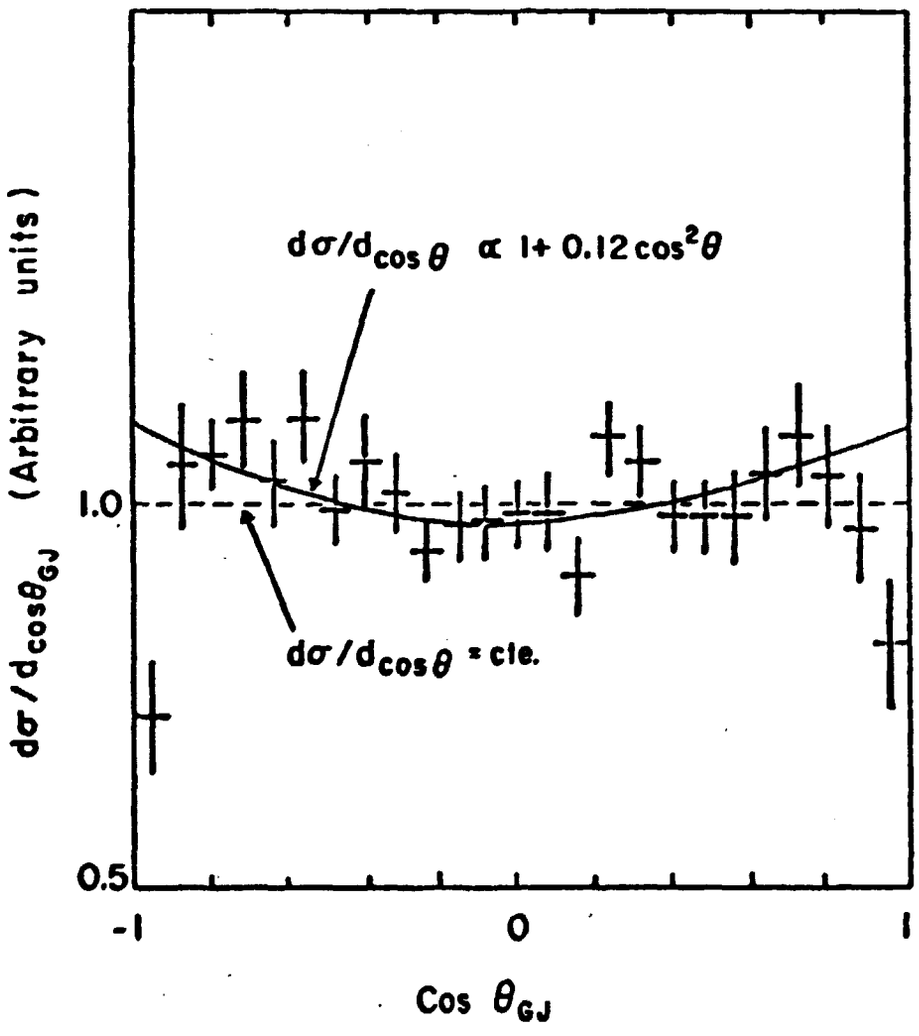

FIG. 11

dσ/dcosθ$_{GJ}$ for J/ψ events from 200 GeV/c π^-'s

A fit c
(9 ± 2 %) cor
gets λ = 0.(
and [12].

This i
the acceptar
the choice
would give

This r
fusion, nor
producing f

II.3.1 Ups

In fig
and π^- at 2
around 9.5
This is the
[16] in pio
nent in the
level of th
fig. 12 th
duced esse
disappears

The a
for the J/
frame. For
dependence
tent with

A fit of λ gives $\lambda = 0.12 \pm 0.05$. If we substract the (9 ± 2 %) continuum contribution ($\lambda = 0.8 \pm 0.2$) [14], one gets $\lambda = 0.05 \pm 0.07$, in very good agreement with refs. [8] and [12].

This isotropic distribution has been used in calculating the acceptance for x and p_t at the ψ, and shows that, for ψ, the choice of the reference axis is not crucial, as all axes would give the same result.

This result is not in contradiction with heavy quark fusion, nor with a model of gluons or light quark fusion producing first a χ resonance decaying into $J/\psi + \gamma$.

II.3.1 Upsilon resonances production : [15]

In figs. 12 and 13 we show the $\mu^+\mu^-$ mass spectra for π^+ and π^- at 200 GeV/c, and for π^- at 280 GeV/c. A clear signal around 9.5 GeV/c^2 is seen in the π^+ induced mass spectrum. This is the first evidence for production of the T state [16] in pion induced reactions. The signals are less prominent in the π^- induced spectra as a consequence of the higher level of the Drell-Yan dimuon continuum. It can be seen from fig. 12 that the background of like-charge muon pairs, produced essentially by π and K decays, is extremely low and disappears above 4 GeV/c^2.

The acceptance for the T was calculated assuming, as for the J/ψ an isotropic decay distribution in the T rest frame. For the Drell-Yan continuum we have taken a $(1 + \cos^2\theta)$ dependence in the Gottfried-Jackson frame, which is consistent with our data (Sect. III.2).

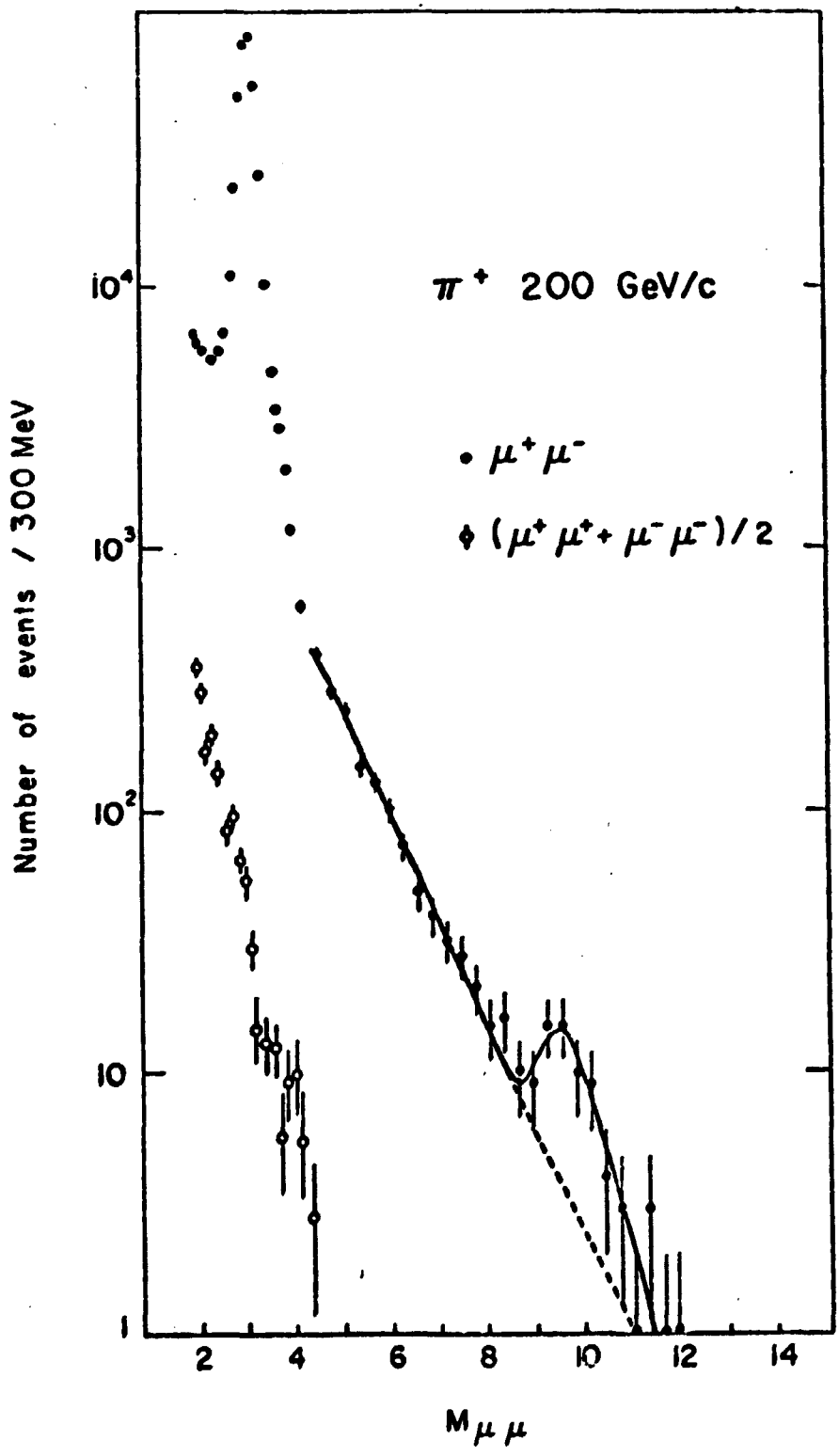

FIG. 12

Dimuon mass spectrum for incident π^+ on a platinum target at 200 GeV/c

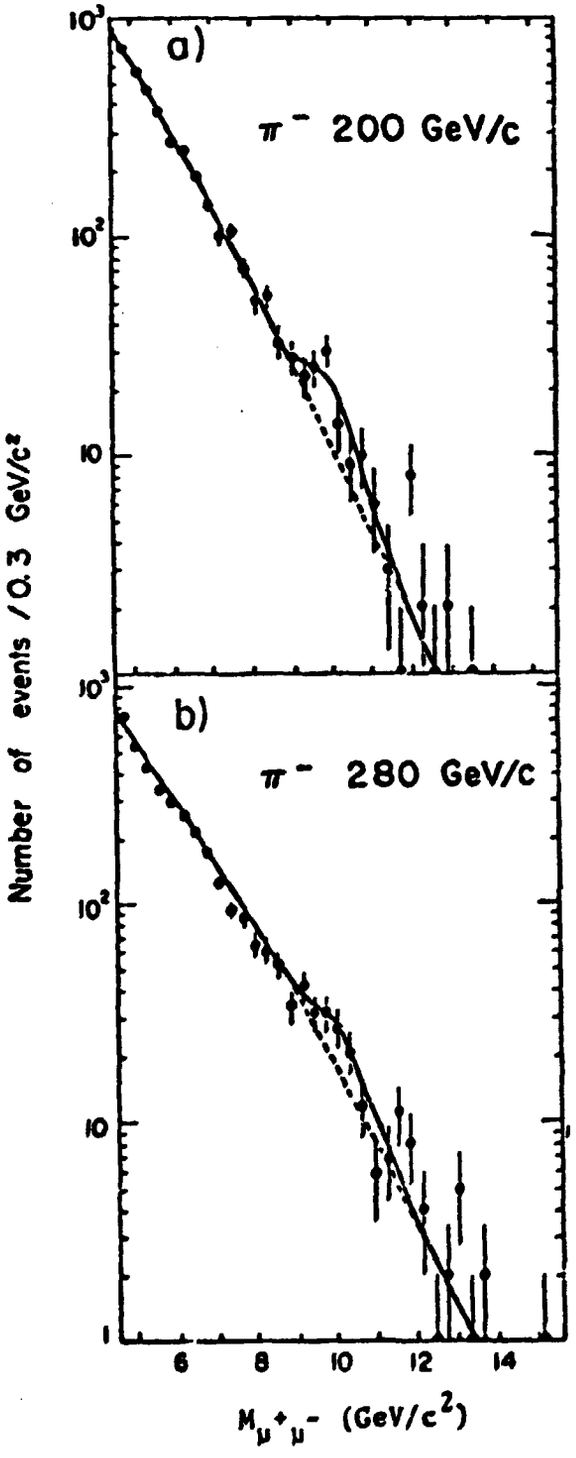

FIG. 13

Dimuon mass spectra in the T region. The curves represent the results of the fits as described in the text

The dimuon mass spectra of figs. 12 and 13 have been fitted to a sum of an exponentially falling continuum, and three Gaussian distributions representing the known T states. The calculated mass acceptance has been folded into the fit. The widths of the three T states, which are not resolved in this experiment, have been fixed equal to the experimental mass resolutions. They were evaluated by a Monte Carlo calculation and found to be σ = 4.5 % at 200 GeV/c and σ = 5.0 % at 280 GeV/c. At the T mass the resolution is dominated by the measurement error on the muon momenta. The masses of the T states were fixed at their known values [17, 18].

Four parameters were left free in the fit :

i) the ratio α of the sum of the three T states to the Drell-Yan continuum at 9.46 GeV/c^2 ;

ii) the relative abundances of the T' and T" states with respect to the T ; these quantities were found to be consistent with the values obtained in proton induced reactions [18] ;

iii) the slope parameter b of the exponential exp(-bM) which describes the continuum.

The fitted values of the parameters α and b are given, together with the total number of events corresponding to the production of all three T states in table 1.

been
m, and
T states.
the fit.
lved in
mental
lo cal-
σ = 5.0 %
ted by
s of
8].

s to the

ates with
consis-
tions

(-bM)

given,
ing to

Table 1

Fitted parameters of the mass spectra of figs. 11 and 12 obtained on a platinum target

Incident particle	π^+ 200 GeV/c	π^- 200 GeV/c	π^- 280 GeV/c
b $(GeV/c^2)^{-1}$	1.055 ± 0.029	0.909 ± 0.016	0.814 ± 0.015
α (GeV/c^2)	4.2 ± 1.0	0.87 ± 0.26	0.70 ± 0.22
$N_T + N_{T'} + N_{T''}$	53 ± 12	55 ± 15	66 ± 20

In table 2 the quantity Bσ (production cross section times the branching ratio into muon pairs) measured in this experiment for the T family is given together with the ratio of T to J/ψ, obtained at the same energies. The cross section per nucleon was evaluated assuming a linear A dependence.

Table 2

Bσ values for T production and for the ratio of T to J/ψ production for different incident particles on a platinum target (systematic errors included)

Particle	π^+ 200 GeV/c	π^- 200 GeV/c	π^- 280 GeV/c
$\frac{B\sigma(T+T'+T'')}{B\sigma(J/\psi)}$	$(2.4 \pm 0.6)\times10^{-4}$	$(1.9 \pm 0.5)\times10^{-4}$	$(2.2 \pm 0.7)\times10^{-4}$
$B\sigma(T+T'+T'')$ (pb/nucleon)	1.9 ± 0.6	1.5 ± 0.5	2.4 ± 0.9
$B\left(\frac{d\sigma}{dy}\right)_{y\approx0.2}(T+T'+T'')$ (pb/nucleon)	2.7 ± 0.9	2.1 ± 0.7	3.4 ± 1.3

The x-distribution for events in the mass range from 8.5 up to 11 GeV/c^2 for incident π^+ at 200 GeV/c is shown in fig. 14. About 2/3 of the events in this mass interval correspond to production of the T resonances. The mean value of x is found to be ∿ 0.2.

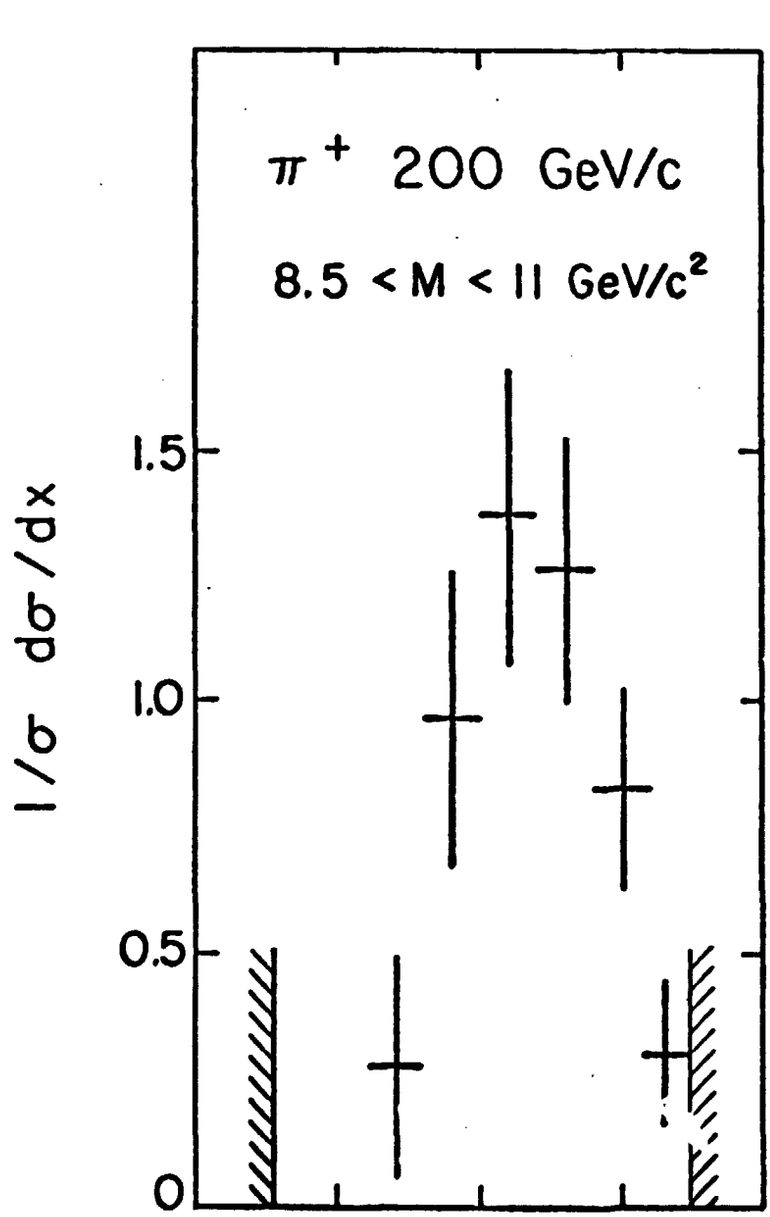

FIG. 14

x-distribution of the events in the mass interval 8.5 < M < 11 GeV/c^2 for π^+ at 200 GeV/c. The kinematical limit is also indicated

For the above sample of events, the decay angular distribution in the Gottfried-Jackson frame was fitted to the expression $1 + \lambda\cos^2\theta$. The best fitted value of the parameter λ was 0.12 ± 0.77 with a $\chi^2 = 1.5$ for 6 degrees of freedom.

We have also made an estimate of the T production by K^+ and protons. The K^+ and p mass spectra were fitted with the same procedure used to extract the T cross section for incident pions. A small excess of events at $M = 9.5$ GeV/c^2 was then found, which leads to the figures given in table 3 for the cross section ratios K^+/π^+ and p/π^+. The corresponding proton cross section can be estimated to be $B\, d\sigma/dy = (3.8 \pm 3.2) \times 10^{-38}$ cm^2/nucleon, assuming a flat y distribution. The results of a model calculation based on the light-quark fusion mechanism, using the structure functions which were obtained from the Drell-Yan analysis of our dimuon data [19, 25] are also indicated in table 3.

Table 3

Cross section ratios for T production at 200 GeV/c. The π^-/π^+ ratio is for a platinum target, while the K^+/π^+ and p/π^+ ratios include events from the platinum target and the dump

	Experiment	Model
$\frac{\sigma(K^+)}{\sigma(\pi^+)}$	0.34 ± 0.23	0.10
$\frac{\sigma(p)}{\sigma(\pi^+)}$	0.03 ± 0.02	0.05
$\frac{\sigma(\pi^-)}{\sigma(\pi^+)}$	0.76 ± 0.29	0.83

eV/c^2

The experimental results are consistent with these predictions. We note that a pure gluon fusion mechanism would give

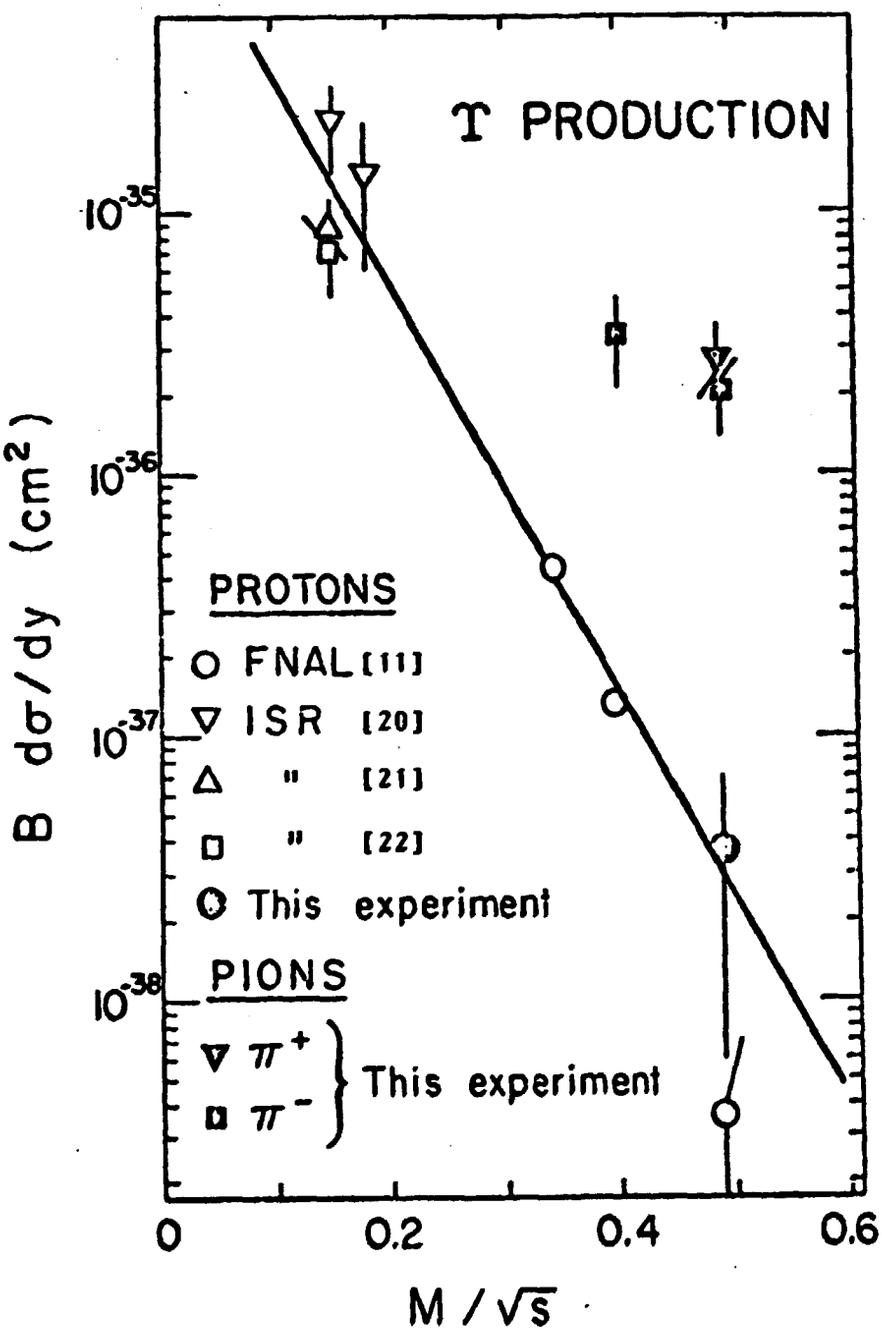

FIG. 15

Differential cross section B dσ/dy for production of the three Υ states plotted as a function of $M/\sqrt{s}$ for incident protons and pions. The FNAL proton data at 300 and 200 GeV are for $y \approx 0.2$ and $y \approx 0.4$, respectively. The pion data of this experiment are for $y \approx 0.2$. Other data are for $y \approx 0$. The line $\exp(-18\ M/\sqrt{s})$ represents an eye fit to the proton data.

about the

π^+, which

Our

15 with p

at FNAL [

[20, 21,

as the rat

protons at

current mo

nation of

nism [23].

In co

effective

GeV/c (M/

sections

the same

peak to t

four. The

of 2.10^{-4}

III DRELL

We h

on a plat

dimuon ev

about the same cross section for T production by K^+ and by π^+, which is not favoured by the data.

Our results for pions and protons are compared in fig. 15 with previous measurements on proton-platinum collisions at FNAL [11] and on proton-proton collisions at the ISR [20, 21, 22]. The energy dependence of T production as well as the ratio of the cross sections for incident pions and protons at a given value of $M/\sqrt{s}$, agree qualitatively with current models using either light-quark fusion or a combination of light-quark fusion and gluon-gluon fusion mechanism [23].

In conclusion, we have shown that pions are much more effective than protons in producing the T states. At 200 GeV/c ($M/\sqrt{s}$ = 0.49), the pion to proton ratio of the T cross sections is of the order of 30. The T cross section is about the same for π^+ and π^-. For incident π^- the ratio of the T peak to the continuum is about one, while for π^+ it is about four. The ratio of the $B\sigma$ values of T to J/ψ is of the order of 2.10^{-4} for incident pions.

III DRELL-YAN CONTINUUM ANALYSIS :

We have measured the production of massive muon pairs on a platinum and hydrogen targets. The following number of dimuon events have been collected for $M > 4$ GeV/c^2.

P_{inc}		π^-	K^-	$\bar{p}$	π^+	K^+	p
200 GeV/c	Pt	5916	119	54	2195	215	1304
	H_2	138	-	-	47	-	24
280 GeV/c	Pt	5700	-	-	-	-	-

ree T states
s. The FNAL
espectively.
are for y = 0.
data.

III.1. Transverse momentum

The fig. 16 displays the mean transverse momentum as a function of the dimuon mass for $\pi^{\pm}$, p at 200 GeV/c and π^- at 280 GeV/c on platinum target. For π^-, one observes a slow increasing with energy (10 % between 200 and 280 GeV/c). At 200 GeV/c, the pion $< p_t >$ reaches about 1.2 GeV/c instead 1 GeV/c for the proton. Furthermore π^+ and π^- data show a similar behaviour.

On hydrogen target, no large deviation is observed relative to the platinum data as presented in the following table.

	π^-	π^+	p
$< p_t >$	1.01 ±0.10	1.17 ±0.20	0.95 ±0.22
$< p_t^2 >$	1.38 ±0.17	1.85 ±0.37	1.11 ±0.30

III.2 Angular distribution :

The angular distribution of the dimuon decay angle is presented in fig. 17 in the Gottfried-Jackson frame. The data are restricted to $p_t < 1$ GeV/c in order to avoid a smearing of the axis, and to $4 < M_{\mu\mu} < 6$ GeV/c^2. A fit of the formulae $1 + \lambda \cos^2\theta^*$ gives $\lambda = 0.80 \pm 0.17$ with a χ^2 of 12.1 for 7 degrees of freedom. A χ^2 of 13.5 is obtained when the value of s is fixed at 1. The Collins-Soper decay angle [24] gives the fitted value : $\lambda = 0.85 \pm 0.17$ with a χ^2 of 10.5. In the Drell-Yan model, these angle definitions are equivalent, since the transverse momentum is not taken into account. Thus, the prediction $\lambda = 1$ is compatible with our data.

$< P_T >$ (GeV/c)

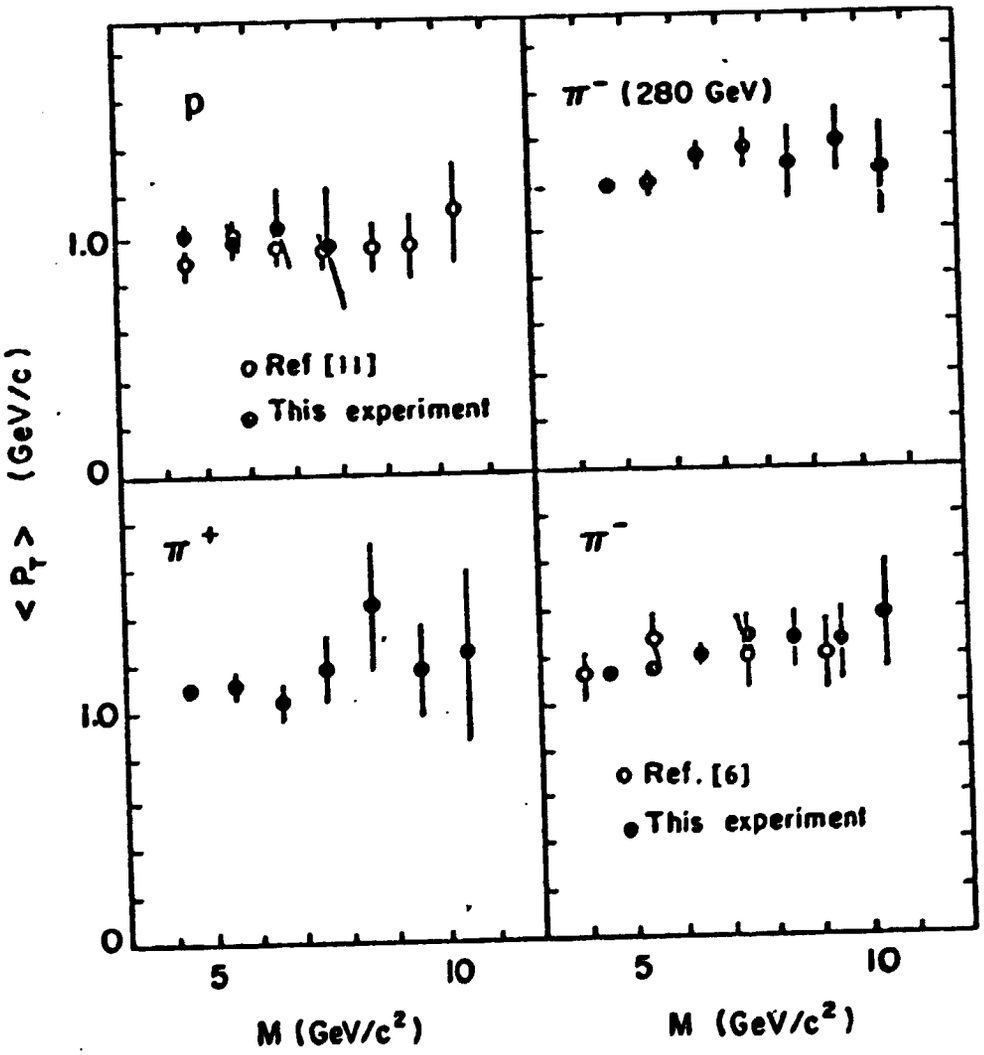

FIG. 16

Mean transverse momentum, as a function of M, for p, π^+ (200 GeV/c) and π^- (280 GeV/c) beams

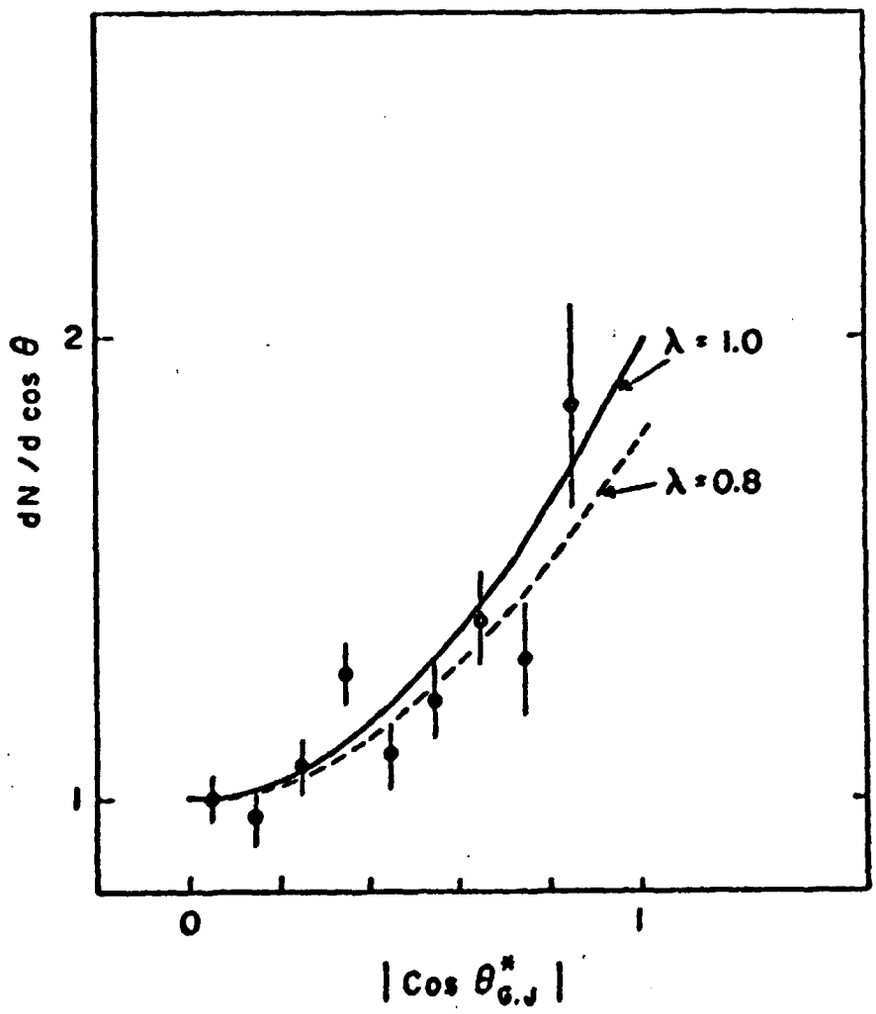

FIG. 17

Distribution of cosθ* (Gottfried-Jackson angle)
for π^- 200 GeV/c, with the cuts $4 < M < 6$ GeV/c^2, $p_t < 1$ GeV/c^2

III.3 The

A com
been made
of the Dre
Details of
Then our a
hypothesis
surements
interactio
ractions [

III.4 Mas

Figs.
incident p
target. Fo
acceptanc
are normal
bars are
error in
due to un
π^+ to π^-
using the

Furt
predictio
the lepto
quark-ant

III.3 The A-dependence

A comparison between our hydrogen and platinum data has been made in order to deduce the nuclear target A dependence of the Drell-Yan continuum cross section parametrized as A^{α}. Details of the analysis are described in another paper [25]. Then our α value is $\alpha = 1.03 \pm 0.03$. This result supports the hypothesis of incoherent proton interactions. Previous measurements of this parameter give $\alpha = 1.02$ for proton-nucleus interactions [26] and $\alpha = 1.12 \pm 0.05$ for pion-nucleus interactions [6].

III.4 Mass spectra :

Figs. 18, 19, 20 show the mass spectra for six different incident particles, measured at $\pm$ 200 GeV/c on the platinum target. For π^- the actual number of events, uncorrected for acceptance is plotted. For the other hadrons the numbers are normalized to the same incident particle flux. The error bars are statistical only, and there remains a systematic error in the relative normalization of $\pm$ 10 % for p, $\bar{p}$, $K^{\pm}$ due to uncertainty in the efficiency of our Cerenkov's. The π^+ to π^- data are normalized at the ψ mass (within $\sim$ 1 %) using the result of Sect. II.2.2.

Furthermore, the mass spectra can be compared to the predictions of the Drell-Yan model [27] which assumes that the lepton pair originates, via a virtual photon, from a quark-antiquark annihilation.

e)
< 1 GeV/c^2

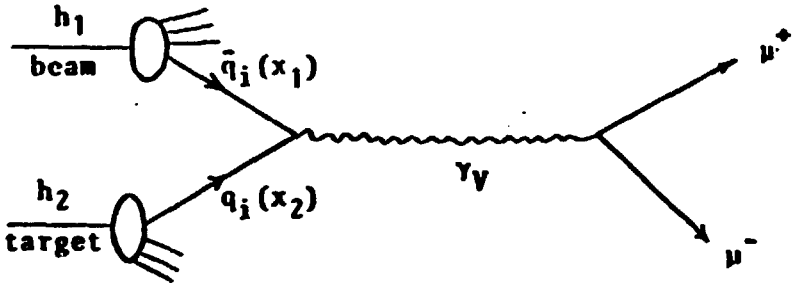

The muon pair mass M and x determine uniquely the momentum fractions x_1 and x_2 of the quark or antiquark coming from the beam and the target :

$$M^2/s = x_1 \cdot x_2 \qquad\qquad x = x_1 - x_2$$

The double differential cross section can be written

$$\left(\frac{d^2\sigma}{dMdx}\right)_{exp} = K \cdot \frac{8\pi\alpha^2}{3M^3} \times \frac{1}{3} \sum_i Q_i \frac{1}{x_1+x_2} \; f_i^{h_1}(x_1)\cdot f_{\bar{i}}^{h_2}(x_2) + f_{\bar{i}}^{h_1}(x_1)\cdot f_i^{h_2}(x_2)$$

where f_i^h and $f_{\bar{i}}^h$ are the structure functions of quark (antiquark) of flavor i with charge Q_i in the hadron h. The factor $\frac{1}{3}$ is due to the color hypothesis. K is a scale factor, related either to our experimental normalization error or (and) to a multiplicative correction factor due to Q.C.D. effects.

The π^+ and π^- data are used to determine the pion and nucleon structure functions. This analysis [25] give the following parametrization :

π^-	valence	$V(x) = 0.55\, x^{0.4}\,(1-x)^{0.9}$
π	sea	$S_\pi(x) = 0.09\,(1-x)^{4.4}$
p	valence up	$u(x) = 10.5\, x^{1.02}\,(1-x)^{4.04}$
p	valence down	$d(x) = 6.3\, x^{1.02}\,(1-x)^{5.04}$
p	sea	$S_N(x) = 0.35\,(1-x)^{6.0}$
	and	$K = 1.4 \quad (\pm 0.5)$

The solid lines of figs. 18, 19, 20 represent the result of the predictions of the model, corrected by our experimental acceptance. We assume the same value of K for the 6 induced

1000
100
10
dN/dM (events/0.5 GeV/c²)
Dimuon ma
Data are
ves are p
Dashed li

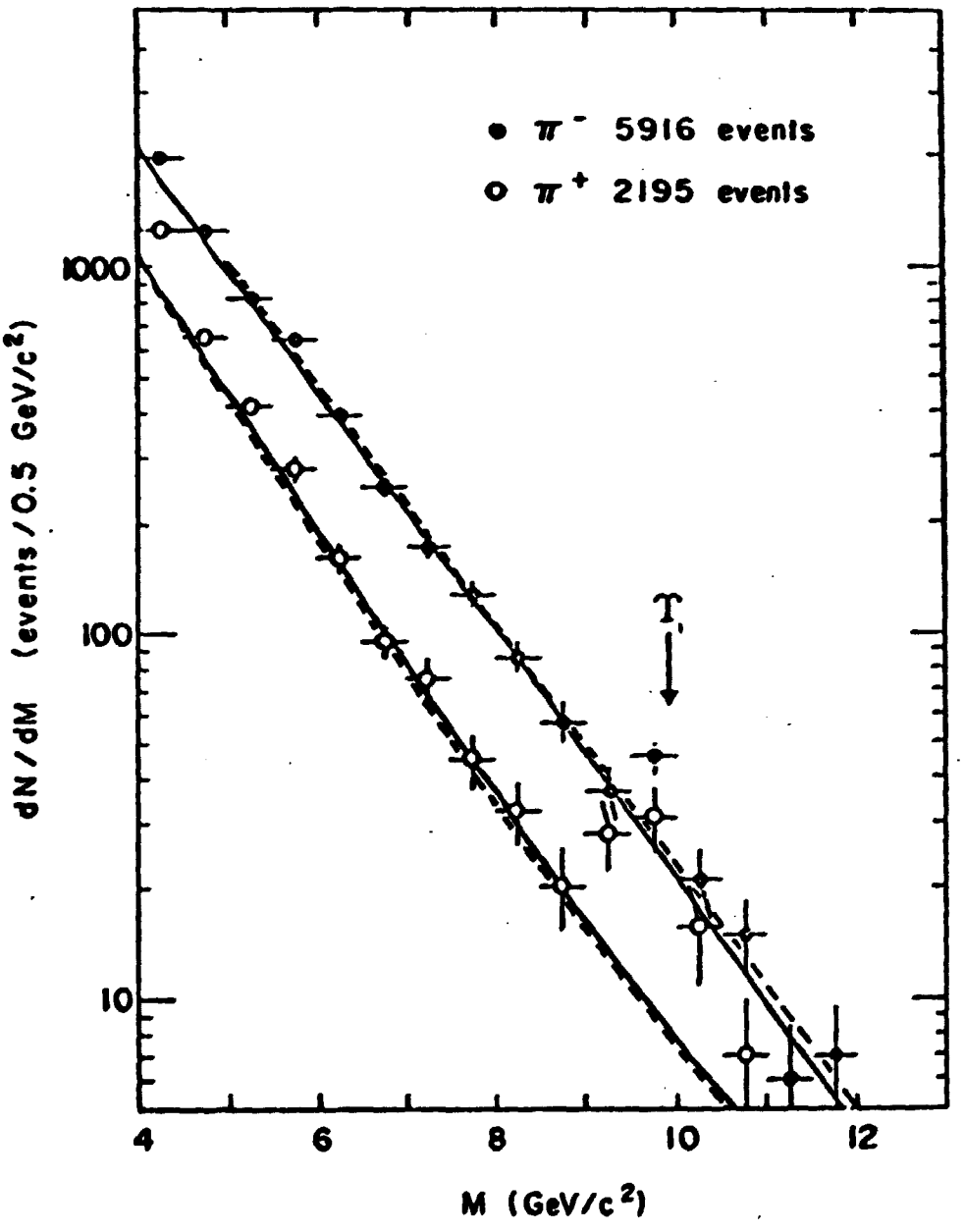

FIG. 18

Dimuon mass spectra induced by $\pi^{\pm}$ not corrected for acceptance. Data are normalized to the same number of beam particles. Curves are predictions of the Drell-Yan model (see text). Dashed lines : CDHS fits used as input.

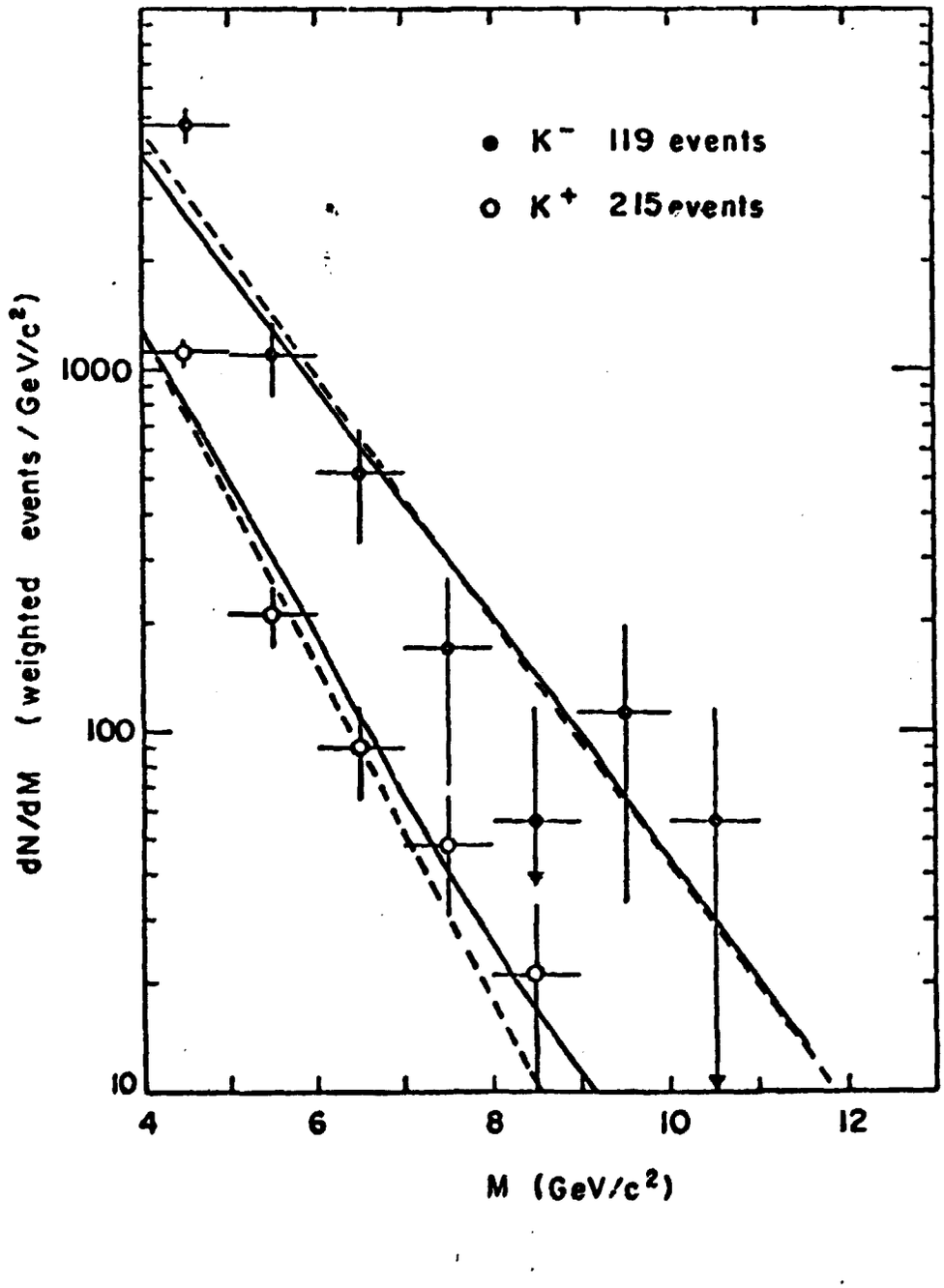

FIG. 19

Dimuon mass spectra induced by $K^{\pm}$

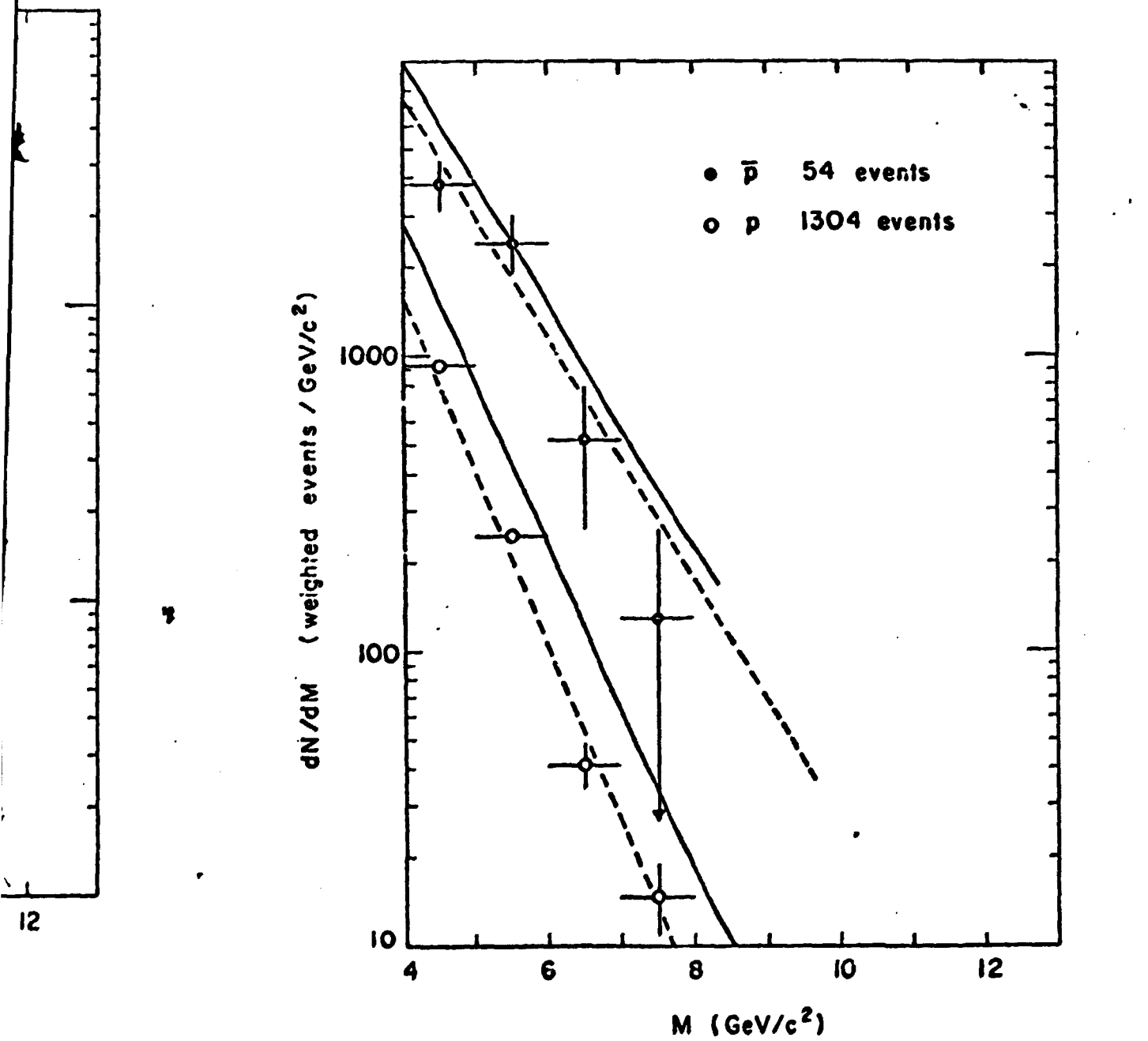

FIG. 20

Dimuon mass spectra induced by p and $\bar{p}$

reactions $\pi^{\pm}$, $K^{\pm}$, $p^{\pm}N \rightarrow (\mu^+\mu^-)X$. We also assume that the pion and proton seas are SU3 symmetric. Furthermore, we suppose exact SU3 invariance to deduce the kaon structure functions from the pion ones.

Besides, we have also displayed in dashed line the expected mass spectra using as input the CDHS nucleon structure functions (at $Q^2 = -20$ GeV^2) in order to determine our π structure functions [25]. In this case we found the scale factor K equal to 2.5.

The π^+ and π^- spectra (fig. 18) shows a relative dimuon production greater for π^- by a factor ~ 3 at high mass excepted in the upsilon region.

One observes that the K^+ induced mass spectrum (fig. 19) is below the K^- spectrum by a factor of 4.5. This could be explained by the fact that the K^- meson contains a valence antiquark $\bar{u}$ which annihilates with the u valence quark of the proton, whereas is the K^+ case, a $\bar{s}$ valence can only fuse with a strange sea quark of the proton. In the SU3 invariance hypothesis, the K^- induced mass spectrum is expected to be equal to π^-. This prediction is compatible with our data, within the present errors.

For incident nucleons p and $\bar{p}$ (fig. 20). The predictions do not fit the data. For the proton the curve is a factor ~ 3 higher than the data points. This discrepancy could be due to a too high value of the nucleon sea, determined from the pion data [25]*. Data taking and analysis of better statistic with $\bar{p}$ are underway.

* But whether or not, the K factor should be the same for meson and for nucleon is an open question.

III.5 Charge asymmetry : $(\sigma_{\pi^+}/\sigma_{\pi^-})$ ratio

A more detailed comparison of the π^+ and π^- spectra is represented by their ratio as shown in fig. 21. This ratio is equal to 1.00 ± 0.01 at the ψ mass, falls toward 0.35 at high mass, except in the upsilon region. A value of $\sigma_{\pi^+}/\sigma_{\pi^-} = \frac{1}{4}$ is expected by the Drell-Yan model for an isoscalar target at large x_1 and x_2 (pion valence antiquark and proton valence quark dominate over the sea). On a platinum target ($Z/A = 0.40$), the value depends of the u/d ratio when $x_2 \to 1$. Thus

Predictions of model	Platinum u/d $x_2 \to 1$	Platinum $\frac{\sigma_{\pi^+}}{\sigma_{\pi^-}}$	Hydrogen $\frac{\sigma_{\pi^+}}{\sigma_{\pi^-}}$
Drell-Yan [27]	2	0.286	0.125
Farrar-Jackson [28]	5	0.327	0.05
Field-Feynmann [29]	∞	0.375	0.0

With the present data, we cannot distinguish between the different predictions.

III.6 Scaling :

The scaling hypothesis states that $M^3 d\sigma/dM$ is a function of M^2/s only. The Drell-Yan model satisfies this property, if the structure functions do not depend on M^2 (the log Q^2 dependence observed in deep inelastic neutrino scattering [30], and predicted by Q.C.D., produces only a very small effect in our $Q^2 = -M^2$ range). Except in the upsilon region (as expected) the scaling property is well satisfied by our data at 200 and 280 GeV/c (fig. 22) within the normalization error of $\pm$ 15 %.

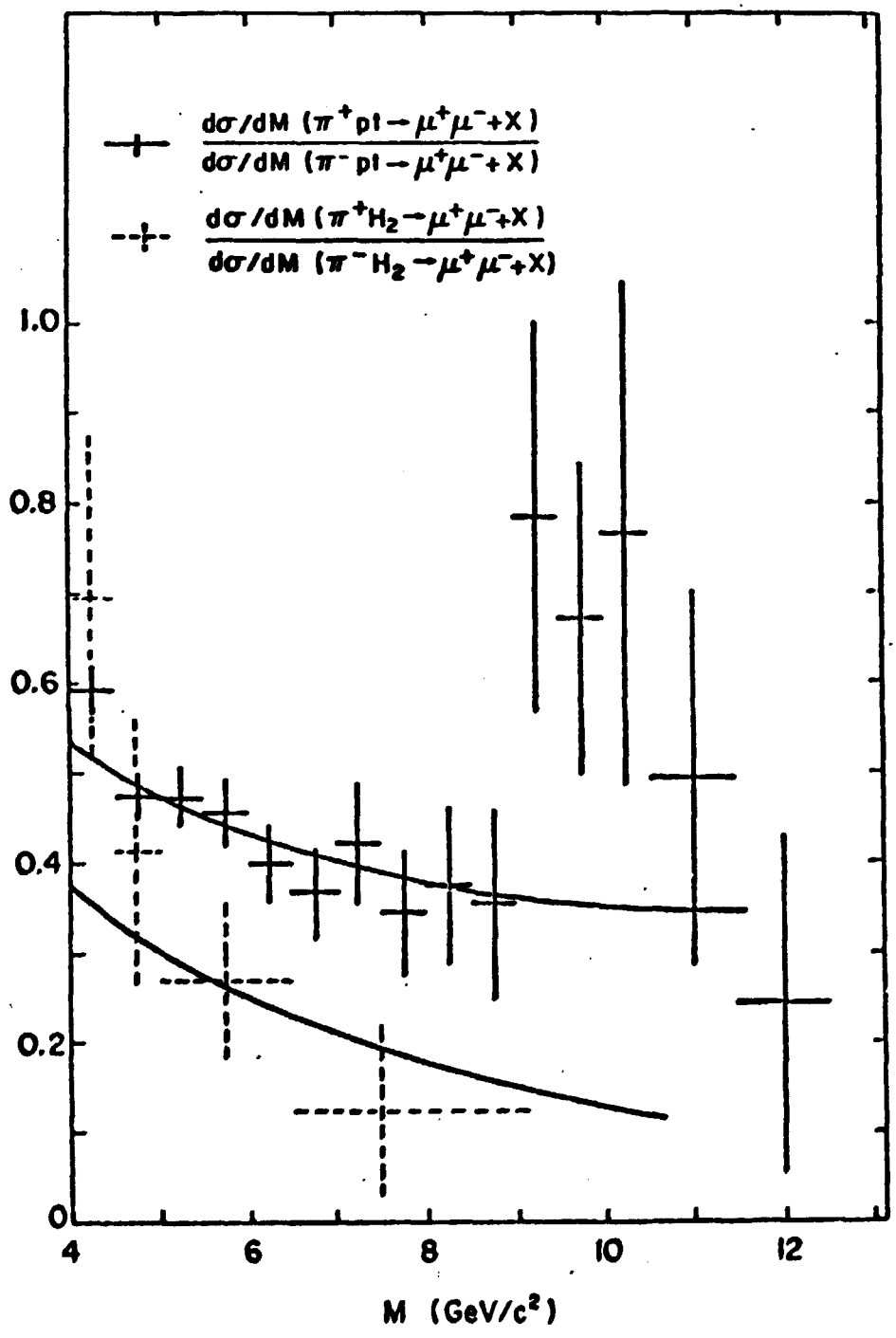

FIG. 21

Ratio of π^+/π^- cross sections, as a function of M, for the platinum and hydrogen targets. The two curves show the predicted ratios $\sigma(\pi^+)/\sigma(\pi^-)$ for the platinum and hydrogen data, respectively, using the structure functions derived from our π data.

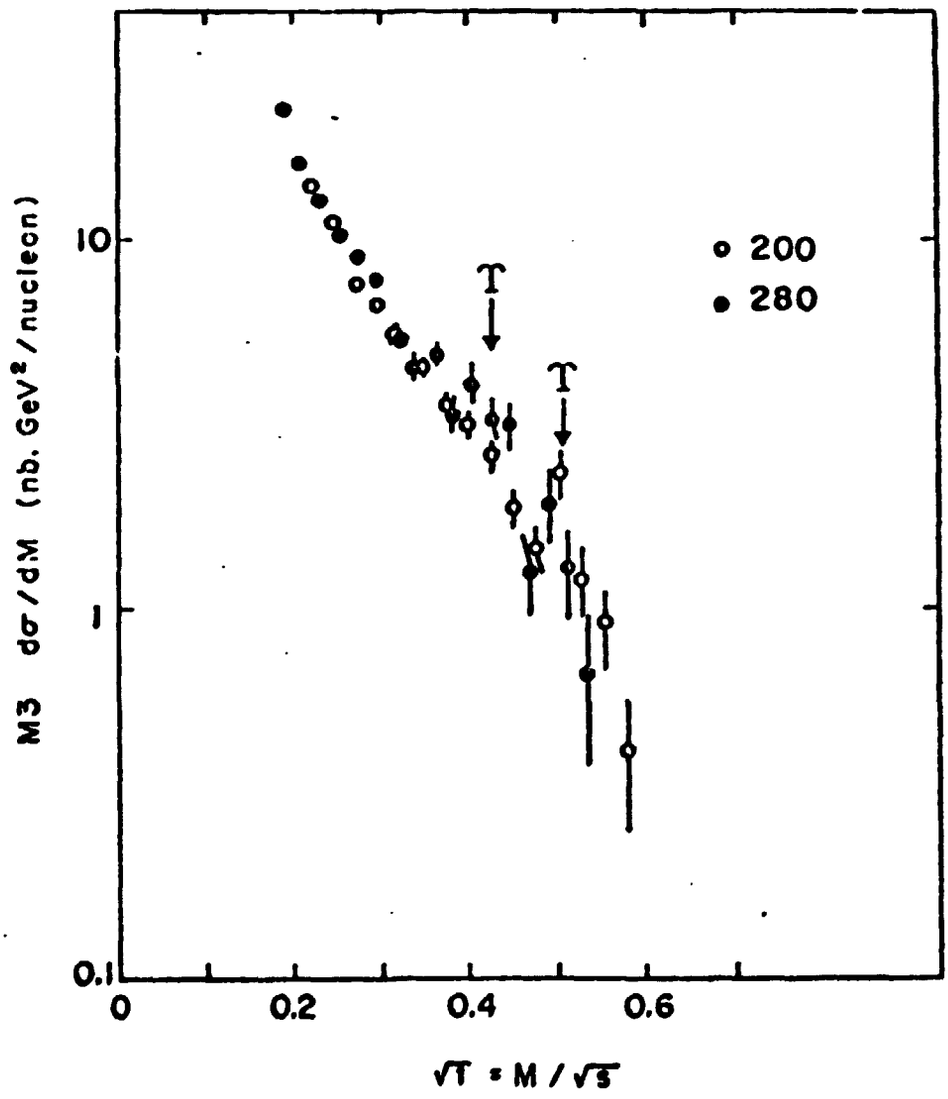

FIG. 22

Plot of $M^3 d\sigma/dM$, as a function of $\sqrt{\tau} = M/\sqrt{s}$ for π^- at 200 and 280 GeV/c^2

platinum and
$\sigma(\pi^+)/\sigma(\pi^-)$
e structure

Comparison with other experiment shows a good compatibility with Goliath π^- data at 150 GeV/c [31]. Difference with data of K.J. Anderson et al. [32] at 225 GeV/c can be due to their result of the A^α dependence : $\alpha = 1.12$.

CONCLUSION

We have measured with a large statistic the production of dimuons on platinum and hydrogen targets by $\pi^\pm$, $K^\pm$, p and $\bar{p}$ beams. New results have been reported on :

A/ Resonance

First observation of UPSILON produced by π^+ and π^- with a relative rate $(\gamma/\psi) \to \mu^+\mu^- \sim 2.10^{-4}$

ψ cross sections measured on HYDROGEN are the same (within 2 %) for π^+ and π^-.

ψ cross sections have been compared for six different incident particle at 200 GeV/c. The ratio of antiproton to proton (1.4 ± 0.2) and K^+ to K^- (1.4 ± 0.2) indicate that PART OF THE ψ IS DUE TO VALENCE QUARK interactions.

x distributions of ψ show a strong difference between incident mesons and baryons, the latter falling more rapidly when x increases. Proton over pion differential cross section falls approximately as $(1-x)^{2.4}$ instead of kaon and pion which have the same behaviour in term of constituant distribution.

B/ Contin

Usi
rim
sha
How
the
p (
σ(π
mas

Sca

Acknowled

I wa
J. Gilman
during th

B/ Continuum

Using the structure functions determined in this experiment with the $\pi^{\pm}$ data, we can roughly reproduce the shape of the MASS SPECTRA for all incident particles. However a constant scale factor K = 1.4, derived from the $\pi^{\pm}$ data, seems to be inadequate to reproduce the p (and possibly $\bar{p}$) mass spectrum in absolute value.

$\sigma(\pi^+)/\sigma(\pi^-)$ falls (on platinum target) $\sim \frac{1}{3}$ at high mass as expected in the quark-parton model.

Scaling hypothesis is well satisfied (within $\pm$ 15 %).

Acknowledgements

I want to thank professors Gary J. Feldman, Frederick J. Gilman and D.W.G.S. Leith for their fair hospitality during this summer Institute.

REFERENCES

[1] C. Bovet et al., IEEE Trans. Nucl. Sci. NS/25 (1978) 572.

[2] J. Badier et al., "NA3 spectrometer", paper in preparation, to be published in Nucl. Instr. and Methods.

[3] M. Morpurgo, "A large superconducting dipole cooled by forced circulation of two phase helium", Cryogenics 19 (1979) 411.

[4] J. Badier et al., "Dimuon resonance production from 200 and 280 GeV/c tagged hadron beam", EPS Intern. Conf. on High Energy Physics, Geneva, 1979.

[5] K.J. Anderson et al., Phys. Rev. Letters 37 (1976) 799.

[6] K.J. Anderson et al., Phys. Rev. Letters 42 (1979) 944.

[7] Y.M. Antipov et al., Phys. Letters 76B (1978) 235.

[8] M.A. Abolins et al., Preprint DPhPE 78-05 ;
M.A. Abolins et al., Phys. Letters 82B (1979) 145.

[9] Y.B. Bushnin et al., Phys. Letters 72B (1977) 269.

[10] M.J. Corden et al., Phys. Letters 68B (1977) 96.

[11] J.K. Yoh et al., Phys. Rev. Letters 41 (1978) 684.
For J/ψ Pt dependence see also
C. Newman, Ph.D. Thesis, Univ. Chicago 1979, unpublished.

[12] J.G. Branson et al., Phys. Rev. Letters 38 (1977) 1331.

[13] S.W. Herb et al., Phys. Rev. Letters 39 (1977) 252.

[14] J. Badier et al., "Muon pair production above 4 GeV (Drell-Yan continuum) by $\pi^{\pm}$, $K^{\pm}$, $\bar{p}$ and p at 200 GeV/c and by π^{-} at 280 GeV/c on platinum and hydrogen targets", Intern. Conf. on High Energy Physics, Geneva, 1979.

[15] J. Badier et al., "First evidence for UPSILON production by pions", to be published in Phys. Letters.

[16] S.W. Herb et al., Phys. Rev. Letters 39 (1977) 252.

[17] J.K. Bienlein et al., Phys. Letters 78B (1978) 360 ;
C.W. Darden et al., Phys. Letters 78B (1978) 364.

[18] K. Ueno et al., Phys. Rev. Letters 42 (1979) 486.

[19] J
p
m
o
p

[20] I
P
T
p

[21] A
o
r
G

[22] L
c
i

[23] J

[24] J

[25] (
I
c

[26] I
J
l

[27]

[28]

[29]

[30]

[31]

[19] J. Badier et al., "Experimental determination of the pion and nucleon structure functions by measuring high-mass muon pairs produced by pions of 200 and 280 GeV/c on a platinum target", EPS Intern. Conf. on High Energy Physics, Geneva, 1979.

[20] I. Mannelli, "Electron pairs production at the ISR", Proc. of the 19th Intern. Conf. on High Energy Physics, Tokyo, 1978, (Physical Society of Japan, Tokyo, 1979), p. 189.

[21] A.L.S. Angelis et al., "A measurement of the production of massive e^+e^- pairs in p-p collisions at $\sqrt{s}$ = 63 GeV, Presented at the EPS Intern. Conf. on High Energy Physics, Geneva, 1979.

[22] D. Antreasyan et al., "Dimuon spectra from 62 GeV proton collisions", presented at the EPS Intern. Conf. on High Energy Physics, Geneva, 1979.

[23] J.F. Owens and E. Reya, Phys. Rev. D17 (1978) 3003.

[24] J.C. Collins and D.E. Soper, Phys. Rev. D16 (1977) 2219.

[25] G. Burgun, "Structure functionsextracted from muon pair production at the S.P.S.", Contribution to the proceeding of the SLAC Summer Institute on Particle Physics (1979).

[26] D.M. Kaplan et al., Phys. Rev. Letters 40 (1978) 435. L.M. Lederman, in proc. of the 19th Intern. Conf. on High Energy Physics, Tokyo, Japan, 1978.

[27] S.D. Drell and T.M. Yan, Phys. Rev. Letters 25 (1970) 316.

[28] G.R. Farrar and D.R. Jackson, Phys. Rev. Letters 35 (1975) 1416.

[29] R.D. Field and R.P. Feynmann, Phys. Rev. D15 (1977) 2590.

[30] J.G.H. de Groot et al., Phys. Letters 82B (1979) 456.

[31] M.A. Abolins et al., "High mass muon pairs produced in π^-Be collisions at 150 and 175 GeV/c". Intern. Conf. on High Energy Physics, Geneva, 1979.